THE ANGLE DEPENDENCE OF THE ROLL DAMPING MOMENT

PETER BENNETT, B Eng

THE ANGLE DEPENDENCE OF THE ROLL DAMPING MOMENT

BY

© PETER BENNETT, B.Eng.

A thesis submitted to the School of Graduate
Studies in partial fulfillment of the
requirements for the degree of
Master of Engineering

Faculty of Engineering and Applied Science
Memorial University of Newfoundland
March 1990

St. John's Newfoundland

ISBN 0-315-61803-5

ABSTRACT

A new approach to the analysis of the free roll decay curve, the Energy method, is examined in this paper and compared with two commonly accepted methods of analysis, the averaging technique of Krylov-Bogoliubov and the Perturbation method. The Energy method uses the equality of the rate of change of the total energy of the system to the rate of energy dissipation due to damping. This method was concluded to be the best method for analysis for three main reasons. 1) It uses the whole roll decay record in its analysis, not just the peak values, allowing for single cycle analysis and analysis of shorter roll decay records. 2) It can separate the influence of the angle and velocity dependent components of the roll damping moment. 3) It can handle non-linear restoring terms which makes it viable for large amplitude motion.

The Energy method and the Krylov-Bogoliubov method were used to analyze stillwater roll decay test records. The results of these analyses indicate a strong angle dependence of the roll damping moment. The quadratic and cubic velocity dependent forms, which are actually functions of the roll angle, of the roll damping moment were shown to be the most viable forms for the roll damping moment. This supports the findings of a strong angle dependence. Stillwater roll decay tests with forward speed were performed and also indicate a strong angle dependence of the roll damping moment. Comparisons of forced roll tests with predictions of forced roll motion using coefficients derived from the stillwater roll decay analyses proved inconclusive.

ACKNOWLEDGEMENTS

I cannot thank my supervisor, Dr. M. R. Haddara, enough for all his support, guidance and patience; possible beatification is not out of the question.

I would like to thank also Dr. D. Bass for his help and the use of his computer programmes.

I wish to extend my thanks and appreciation to Dr. T. Chari for his consideration with respect to funding and teaching assistantships.

I thank Dr. D. Muggeridge for the use of the wave tank and its facilities and I give heartfelt thanks to Mike Sullivan, Blair Wilkie, Wayne Brown and Lloyd Little for their unstinting efforts to ensure accurate reliable results and for their sanity saving blend of professionalism and humour.

Mrs. Moya Crocker deserves a medal for her patience and good humour in dealing with the general idiocies of graduate students and Mrs. Mary Brown has ensured her place in heaven, if my vote counts at all, for her efficient and accurate typing at short notice.

A thousand thanks to Mohan and Stuart for your generous help in a dark hour of need.

Last and certainly not least, I want to thank my wife, Sheila, for her patience, love and perseverance in motivating me.

TABLE OF CONTENTS

TABLE OF CONTENTS

LIST OF FIGURES

LIST OF FIGURES (cont'd)

LIST OF FIGURES (cont'd)

LIST OF FIGURES (cont'd)

LIST OF TABLES

LIST OF TABLES (cont'd)

1.0 INTRODUCTION

Rolling motion is the most crucial and yet most difficult to predict of all ship motions. If the roll damping moment of a vessel is underestimated, under certain conditions, this could lead to capsizing and possible loss of life or vessel. These consequences have led to a considerable amount of investigation into rolling motion over the last century. Various kinds of roll damping devices have been proposed, both active and passive, from the simple addition of bilge keels to anti roll devices such as flume tanks or gyroscopically stabilized vessels. One of the most effective and least expensive devices has been the bilge keel; basically a flat plate affixed normal to the hull at the turn of the bilge and running parallel to the streamlines. Byran [30] and Gawn [6] investigated this device in the early part of this century. More recently, Bolton [21] investigated the effects of size and placement of bilge keels on roll reduction. Lugovski et al [22] performed a study examining the scale effect of bilge keels and determined, not unreasonably, that the size of the vessel used in the experiment has a direct effect on the scale effect of the bilge keels. The scale effect arises due to the large viscosity dependent component of damping due to the bilge keels.

The amount of interest in rolling motion has also generated considerable speculation as to the form of the roll damping moment. It

has long been accepted that the equation of rolling motion is comprised of an inertial term related to the angular acceleration of roll, a damping term related to the angular velocity of roll, a restoring term related to the angle of roll and an exciting moment term. It has also long been realized that the damping moment and the restoring term are generally nonlinear. Froude [1] is credited with advancing the formulation of the linear plus quadratic velocity dependent damping moment. This formulation has been used almost exclusively for the last century. Since Froude, many theoretical and experimental studies have been performed concerning the rolling motion and roll damping of ships. The "Strip Method" has made possible the calculations, with reasonable accuracy, of all the terms in ship motion equations except for the roll damping term. The nonlinear characteristics of roll damping, due mainly to the effects of fluid viscosity, as well as its strong dependence on forward speed, make the prediction of roll damping so difficult. The fact that, in the absence of bilge keels, the influence of these effects on the roll damping are of the same order of magnitude further complicates matters. An extensive series of tests at zero ship speed were carried out in 1957 by Watanabe and Inoue (as reported by Himeno [11]) and at forward speed by Yamanouchi (as reported by Himeno [11]) in 1961. The fact that the results from these tests are used up to the present time points out the difficulty of treating the problem of roll damping rigorously.

Not until the 1970's was an acceptable alternative provided for the classical linear plus quadratic velocity dependent roll damping moment. Haddara [2] introduced the linear plus cubic velocity dependent damping moment to overcome analytical difficulties arising from the use of the quadratic form. Dalzell [4] performed a detailed study on the cubic term which indicated that the cubic model was both quantitatively and qualitatively reasonable within the range and scatter of available experimental data.

Haddara [3] performed a further study of the form of the roll damping which showed that different models may be obtained for the same roll decay data. These different models would fit the data to within the same degree of accuracy but would predict different rolling motion responses outside the range of data. It was suggested that a criterion for the selection of a model be how well it predicts the roll response outside the range of data, not how well it fits the data.

Although studies such as Spouge et al. [5] indicate that there is an angle dependent component to the roll damping moment, this form of dependence has not been studied in detail. Watanabe and Inoue (as

reported by Himeno [11]) also note this type of dependence in the form of an amplitude.

The absence of an appropriate analysis tool seems to be the main reason behind this lack of studies into the angle dependence of the roll damping moment. The averaging technique is frequently used in the analysis of roll decay records but cannot separate the influence of angle dependent and velocity dependent components of the same order of magnitude.

Until recently, there were two main types of analyses. The first uses the method of slowly varying parameters and is known as the averaging technique of Krylov-Bogoliubov [4,3,8]. The second uses a perturbation technique.

Dalzell [4] investigated the cubic and quadratic models using the method of slowly varying parameters and a least squares technique to find an equation for the rate of decay of the peaks of the roll decay curve as a function of the damping moment parameters. Haddara [3] used a stochastic version of the same technique to investigate various models including angle dependent forms. The method was accurate and easy to apply but could not separate the influence of the angle dependent and

velocity dependent components of the same order of magnitude. The method was only suitable for linear restoring moments which is unrealistic for large amplitude motion.

Roberts [8] related the parameters of the roll damping moment, including the amplitude of rolling motion, to a loss function using a stochastic approach. Experimental values were obtained for the loss function and used to derive the parameters of the roll damping moment by means of a least squares technique. A spline fitted to the peaks of the roll decay curve was used to obtain experimental estimates for the loss function. The method is suitable for use with a nonlinear restoring moment, but, because the averaging technique was used, the method fails to identify the angle dependent components of the same order of magnitude as the velocity dependent components.

Mathisen and Price [9] used a perturbation method to identify the roll damping parameters and to approximate the free rolling response of a vessel. This method assumes that the nonlinear response is a small perturbation of the linear response which makes the method valid for small nonlinearities only. The method also assumes small linear damping and is capable of handling simple forms of nonlinear damping moments and linear restoring moments only.

All of the above mentioned techniques share one main disadvantage. They all require the use of only the peak values of the roll decay curve in the measurement and fitting of the roll damping moment. This necessitates the use of relatively long roll decay records for a reasonably accurate fit. These records are usually difficult to obtain, especially if the influence of bilge keels is being investigated. As well, the latter part of the roll decay curve, ie. at smaller amplitudes, is of doubtful accuracy.

Recently, two techniques were introduced by Bass and Haddara [7], the Energy method and the DEFIT method, which could separate the influence of all the components of the roll damping moment. The Energy method, so named as its analysis is predicated on the equality of the rate of change of the total energy of a system to the rate of energy dissipated by damping, allows for single cycle analysis of roll decay records. Such analysis would provide new insight into the damping terms as the roll angle decreases.

The following investigation used this Energy method to analyze the roll decay records of a set of experiments performed in the wave tank at Memorial University of Newfoundland. Comparisons with two accepted methods, the Krylov-Bogoliubov method and the Perturbation method, are carried out as a check of the validity of the Energy method. The subsequent

single cycle and whole cycle analyses are used to determine if angle dependent terms are appropriate in the roll damping moment. The Energy method is also used to investigate the effect of forward speed on free roll damping.

A further check on the validity of the derived damping forms is performed by comparing the predicted forced roll response, using the roll damping coefficients obtained from the Energy method analysis, with experimental values of the forced roll response.

2.0 EXPERIMENTAL STUDY

Two sets of tests, conducted one year apart, were performed in a wave tank at a water depth of approximately 2.0 metres. The tank measures 58.27 metres long, 4.57 metres wide and 3.00 metres deep. Waves are created by an MTS servohydraulic piston type wave generator at one end. At the other end is a parabolic shaped wave absorbing beach to reduce reflected and standing waves. The wave generator is a closed loop device, capable of producing both regular (sinusoidal) or irregular (random) waves. The irregular waves can be based on different theoretical models such as Neumann, Pierson-Moskowitz, JONSWAP, etc. The generator receives the sinusoidal function from a simple function generator capable of producing sinusoidal waveforms. The irregular wave forms are entered into the generator after a wave spectrum has been transformed into a time series using the HP-86 microcomputer.

A towing carriage runs on parallel rails 4.88 metres apart on top of the tank walls and is capable of speeds from 0 to 5 m/s. The towing carriage is equipped with a towing dynamometer with a freely moving heave post. An angular induction transducer can be attached to the heave post in order to measure rotations about a horizontal axis. The carriage

operating platform can be raised or lowered to facilitate testing at different water depths.

In the first set of tests, two ship models, the M.V. Arctic and an R-class icebreaker, were subjected to roll decay tests in still water and forced roll in regular beam seas. For the forced roll tests, a range of wave frequencies straddling the model roll natural frequency was chosen. For each frequency chosen, tests were performed with three different moments of inertia for the ship model.

In the second set of tests an R-class icebreaker was subjected to roll decay tests in still water and forced roll tests in both regular and irregular seas. Again, for the forced roll tests, a range of frequencies straddling the natural frequency of roll was chosen. Each test was performed for the ship model without bilge keels, with bilge keels and with bilge keels and a 10% increase in the moment of inertia.

Spouge, Collins and Ireland [5] discuss methods of various complexity for the performance of roll decay tests. It is desirable to have as pure an initial roll exciting moment as possible. This was considered prior to the performance of the roll tests on the M.V. Arctic model and the R-Class icebreaker model. However, due partly to financial and material

constraints and partly to the fact that rolling motion is coupled with the other degrees of freedom to a certain extent anyway, it was decided to impress the initial heeling moment manually. Concerns over manually heeling a model are that pushing one side of the vessel down and releasing it would produce a heave response as well as a roll response. Due to the coupling between heave and roll, this heaving motion would interfere with the roll response and accurate results would not be possible. To overcome this, one side of the vessel was pushed down while the other side was pulled up with approximately the same force. This produces a purer heeling moment with correspondingly less heave response. With a little practice, the experimenter can become adept at judging the balance of forces. The SELSPOT system's ability to measure the six degrees of freedom of the response corroborated the decision to use this method. Acceptable confidence intervals using the linearized damping coefficients were calculated.

In the first set of tests, the forced roll tests were performed with the model tethered and untethered. It was found that insufficient data could be collected with the model untethered due to the amount of drift. Consequently, further forced roll tests were performed with the model tethered. The tethering points were made to be contained in the longitudinal axis containing the centre of gravity. The tethering rods are described in the following section.

2.1 The Models

Two models were used to obtain roll data. A 1:80 scale model of the M.V. Arctic and a 1:40 scale model of an R-Class icebreaker hull form. Both models were previously built according to specifications of the Institute for Marine Dynamics. The M.V. Arctic model was built at the Institute for Marine Dynamics on their numerically controlled milling machine. The R-Class icebreaker model was built at the Cabot Institute using a lines plan and parameters supplied by the Institute for Marine Dynamics.

For the first set of tests, the moments of inertia and centres of gravity of the M.V. Arctic and the R-Class icebreaker were chosen arbitrarily, as no data concerning these parameters were available at the time.

For the second set of tests, data concerning a typical condition, including a typical roll period, for the R-Class icebreaker were obtained from the Institute for Marine Dynamics and used.

The models were ballasted and trimmed to the correct waterlines as indicated on the specification sheets from the Institute for Marine Dynamics. Sets of weights were arranged in each model such that they could be moved together or apart in a horizontal plane, thereby allowing the roll moment of inertia to be changed without changing the vertical centre of gravity, to see the influence of the roll natural frequency on damping. These arrangements allowed for a maximum change in the roll moment of inertia of approximately 7% for the M.V. Arctic, approximately 18% for the R-Class icebreaker in the first set of tests and approximately 10% for the R-Class icebreaker in the second set of tests.

2.1.1 The M.V. Arctic Model

The M.V. Arctic model was constructed of laminated wood milled to the correct shape and hollowed to a shell thickness of approximately 3 cm. The outer hull was then covered with an epoxy coating and smoothed. There was no deck.

A body plan of the model is given in Fig. 2.1.1.1. The particulars of the model are given in Table 2.1.1.1.

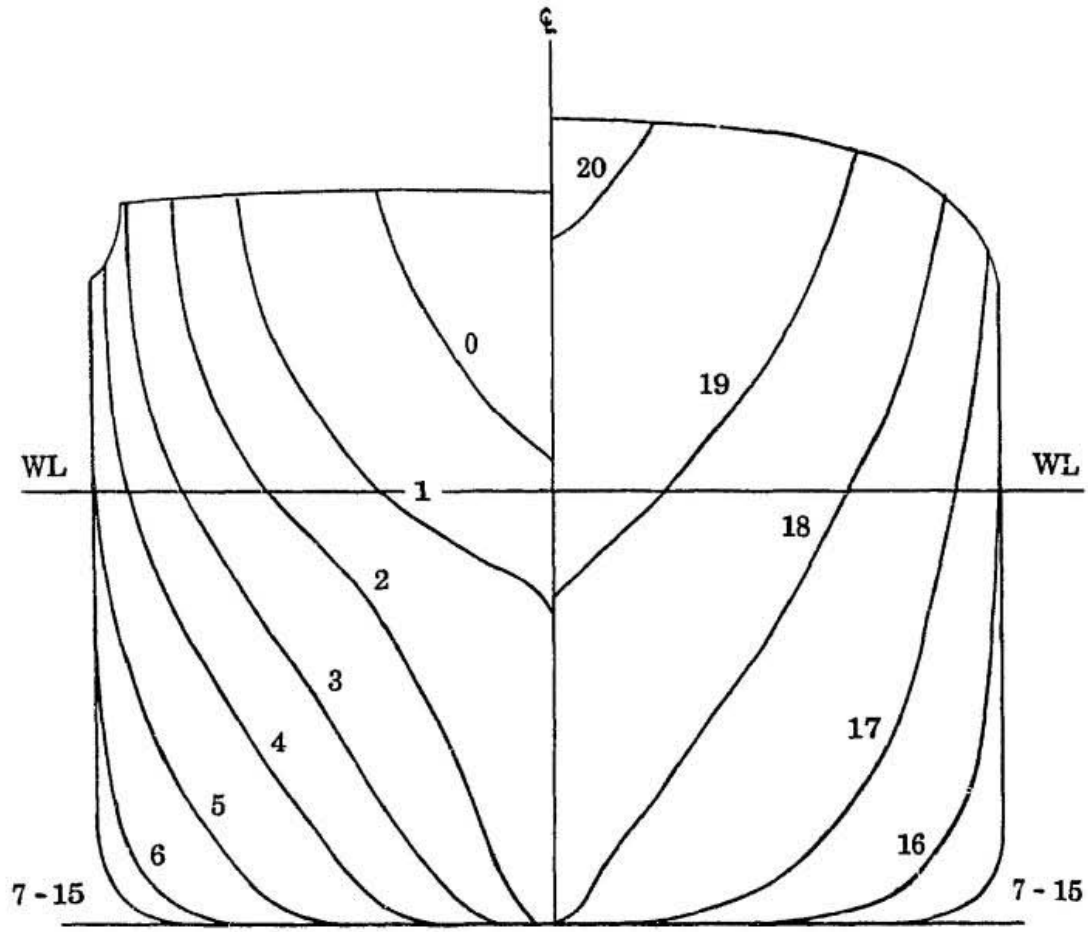

Figure 2.1.1.1
Body plan of M.V. Arctic

TABLE 2.1.1.1

M. V. "ARCTIC" Model Particulars

Scale 1:80

L.B.P.	2.456 m.
BEAM	0.2857 m.
DEPTH at midships	0.204 m.
DRAFT	0.1371 m.
DISPLACEMENT	70.20 kg
V.C.G. above Baseline	0.096 m.
L.C.G. from A.P	1.270 m.
GM	0.0292 m.

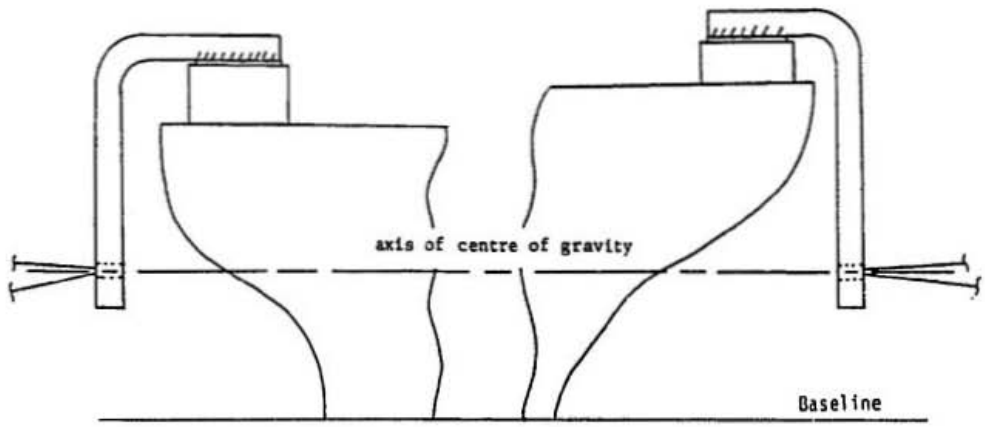

TETHERING ARRANGEMENT

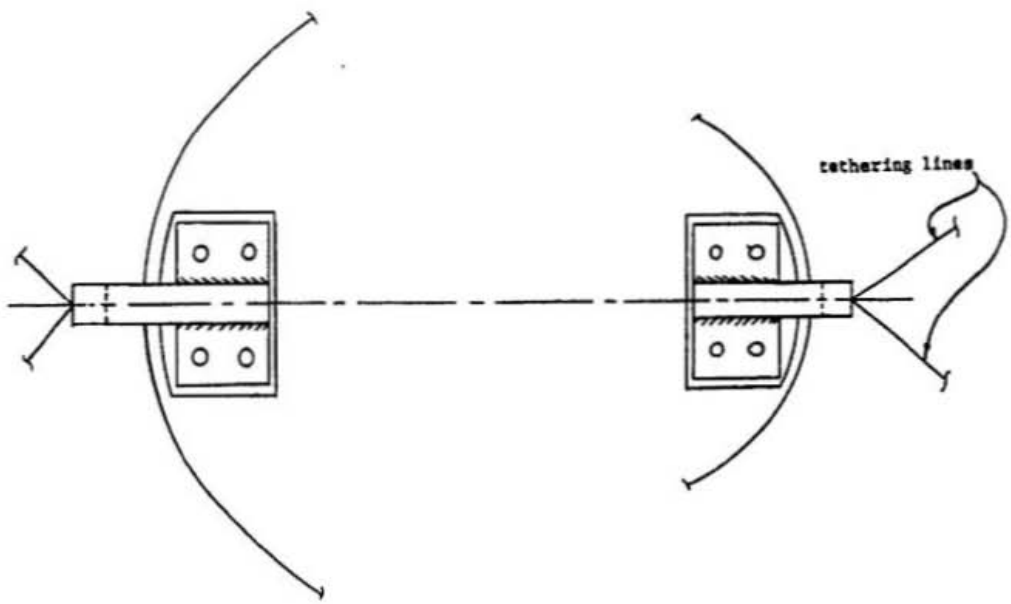

Figure 2.1.1.2
Tethering arrangement for forced roll tests

of gravity. Tethering rods of 1/4 inch mild steel were bent into an L shape and fitted at bow and stern. The tethering point on the rod was determined by laying the model on a level surface and measuring from the surface to a point on the rod equivalent to the height of the centre of gravity. See Fig. 2.1.1.2

2.1.2 The R-Class Icebreaker Model

The R-Class icebreaker model was constructed of fibreglass woven roving impregnated with epoxy resin for the shell, with 1/4 inch plywood covered with epoxy resin for the two bulkheads and the deck. The outer hull was covered with gel coat and smoothed.

A body plan of the model is given in Fig. 2.1.2.1. The particulars of the model for each set of tests are given in Tables 2.1.2.1 and 2.1.2.2.

For the tethering of the model for the forced roll tests, 1/2 inch mild steel rods were used, bent into an L shape and attached at bow and stern. The assumptions and methods for determining the tethering points used for the M.V. Arctic were used for the R-Class icebreaker as well.

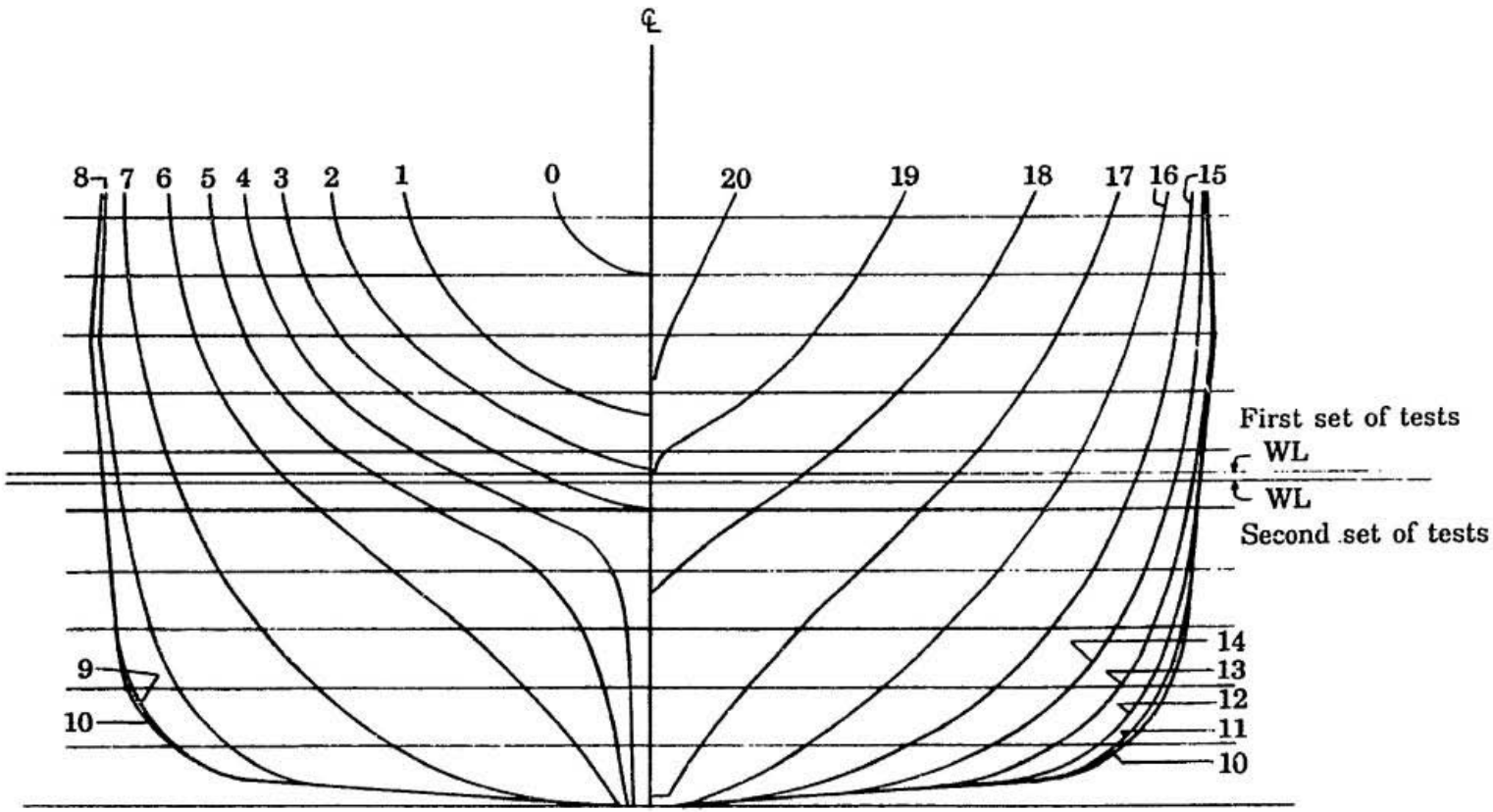

Figure 2.1.2.1
Body plan of R-Class icebreaker

TABLE 2.1.2.1

R-Class Icebreaker Model Particulars
(First set of tests)

Scale 1:40

L.B.P.	2.192 m.
BEAM	0.484 m.
DEPTH at midships	0.310 m.
DRAFT	0.1785 m.
DISPLACEMENT	122.0 kg
V.C.G. above Baseline	0.055 m.
L.C.G. from A.P.	1.107 m.
GM	0.086 m.

TABLE 2.1.2.2

R-Class Icebreaker Model Particulars
(Second set of tests)

Scale 1:40

L.B.P.	2.192 m.
BEAM	0.484 m.
DEPTH at midships	0.310 m.
DRAFT	0.1735 m.
DISPLACEMENT	117.6 kg
V.C.G. above Baseline	0.1936 m.
L.C.G. from A.P.	1.107 m.
GM	0.025 m.

2.1.3 Calculation of the Centres of Gravity of the Models

Two methods were used to calculate the centres of gravity of the two models. The first used a frame balance to determine the centre of gravity directly; the second used an inclining experiment and the hydrostatic particulars of the models.

For the first set of tests, the centres of gravity of the models were chosen arbitrarily. Therefore, the models were ballasted and trimmed to even keel and the resultant centres of gravity measured. For the second set of tests, the vertical centre of gravity and the natural period of roll of the R-Class icebreaker were to be modelled to suit the parameters obtained from the Institute of Marine Dynamics. This required a number of iterations of ballasting and measurement of the centre of gravity and roll period.

2.1.4 Frame Balance

The frame balance consists of a rigid outer frame supporting a rigid inner frame on two knife edges such that the inner frame is free to swing. See Fig. 2.1.4.1. The inner frame has a platform upon which the model can be laid.

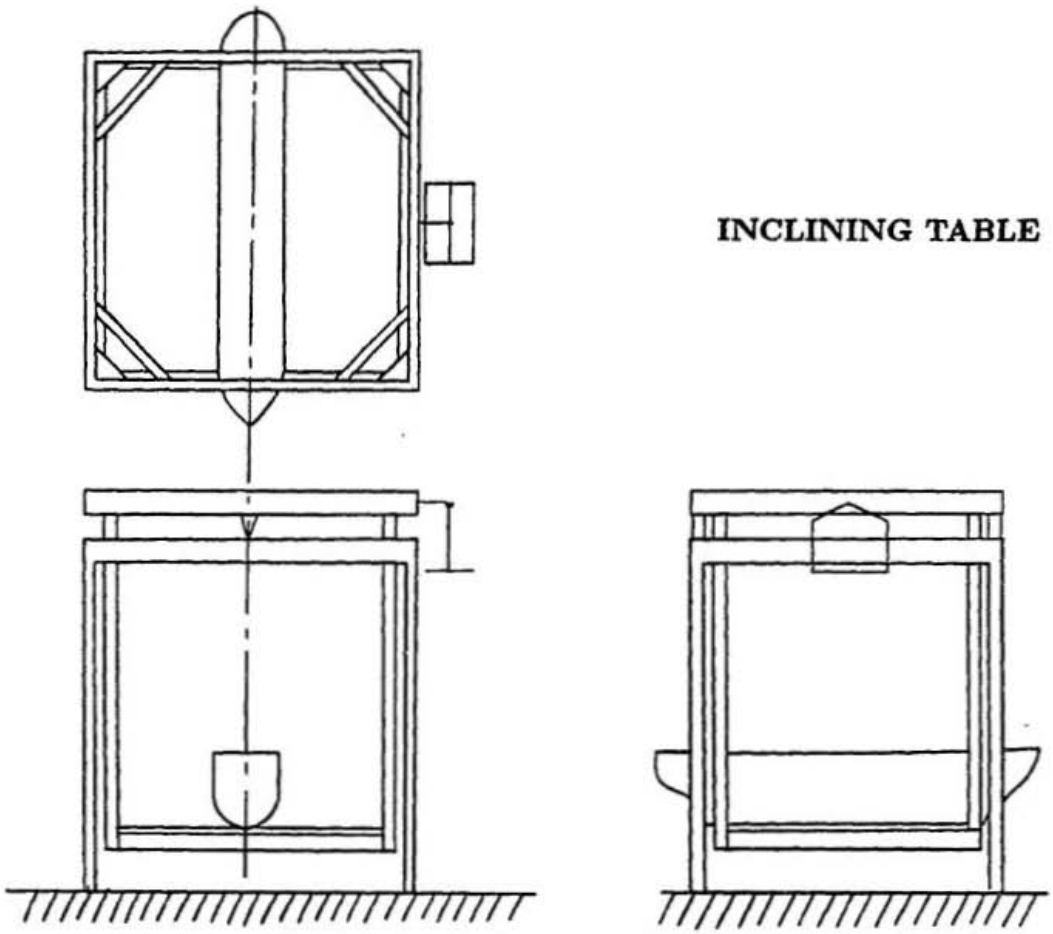

Figure 2.1.4.1
Plan, front and profile views of inclining table

The empty inner frame is levelled with a bubble level and the distance between inner frame and outer frame is measured with Vernier calipers at a known distance from the axis formed by the two knife edges. Subsequent deflection measurements are taken at the same point.

Weights are added to a pan which had been suspended from the inner frame at a known distance from the axis formed by the knife edges previous to the levelling of the inner frame. The addition of the weights causes the inner frame to rotate relative to the outer frame and the deflections are measured at the previously mentioned point. The weights are incremented to give a range of deflections up to a maximum of approximately 3.5 degrees rotation.

The weights are then removed from the pan and the initial distance from inner to outer frame is checked.

The model is then placed upon the inner frame platform and adjusted until its centre of gravity lies in the same vertical plane as the inner frame's centre of gravity. This is achieved by adjusting the model until the distance from inner to outer frame is the same as the distance when the inner frame was empty. Weights are again added to the pan and a range of deflections are recorded.

Linear regression techniques are used to determine equations describing the plots of the tangent of the deflected angle (deflection/distance to knife edge axis) versus the added moment for both the empty frame and the frame plus model. Choosing an angle within the data range, values for the added moment for both the empty frame and for the frame plus model are obtained. Subtracting the added moment for the empty frame from the added moment for the frame plus model will give the restoring moment provided by the model. The vertical centre of gravity of the model can then be calculated using the following formula:

$$CG_m = H - \frac{M_m}{W_m \tan\theta} \qquad 2.1.4.1$$

where
- H = the distance from knife edge axis to the platform
- M_m = restoring moment due to the model
- W_m = weight of model
- CG_m = vertical centre of gravity of the model

2.1.5 The Inclining Experiment

An inclining experiment was performed on each model, for each set of tests, as a check.

Four known weights were moved transversely a known distance and the resultant inclination of the model was measured for each movement using a digital inclinometer. The metacentric height, GM, was calculated for each inclination and the results were averaged.

The following equation was used to determine the metacentric height, GM.

$$GM = \frac{M}{W_m \tan\theta} \qquad 2.1.5.1$$

where
M = the inclining moment
W_m = the displacement of the model (weight)
θ = the induced angle of inclination

The vertical centre of gravity was calculated using the following formula:

$$KG = KB + BM - GM \qquad 2.1.5.2$$

where
KG = vertical centre of gravity
KB = vertical centre of buoyancy
BM = distance from vertical centre of buoyancy to metacentre
GM = distance from vertical centre of gravity to metacentre
= metacentric height

KB and GM were taken from the hydrostatic particulars supplied by the Institute for Marine Dynamics.

In order to determine a nonlinear equation for the restoring moment to be used in the Energy method, values of the righting lever arm for various angles, or a GZ curve, had to be deduced. The Wolfson Unit MTIA Hydrostatic and Stability software package was used for this purpose. The set of offsets describing the hull of the model and various other parameters were input to this package which then calculated the GZ curve values. (See Figs. 2.1.5.1, 2.1.5.2, 2.1.5.3). A least squares routine was then used to fit a polynomial to these values. The GZ curve is symmetric about the origin of the axes and therefore the righting lever arm will vary from positive to negative as the roll angle varies from negative to positive. This is accomplished by having the terms of the restoring moment raised to odd powers only.

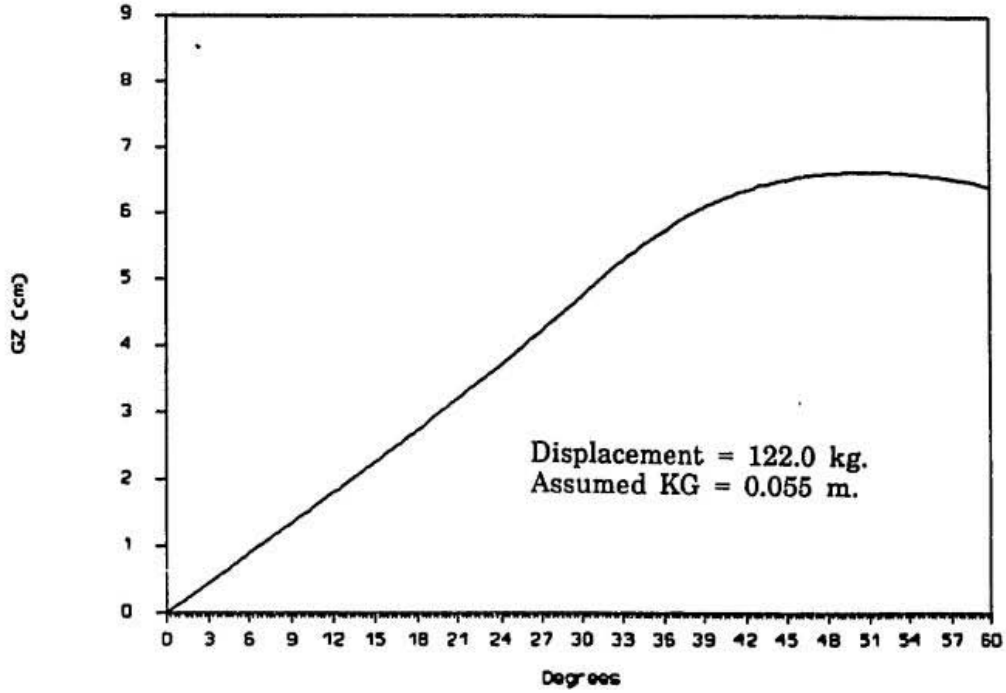

Figure 2.1.5.1
Restoring lever arm, GZ, curve for R-Class icebreaker in first set of tests

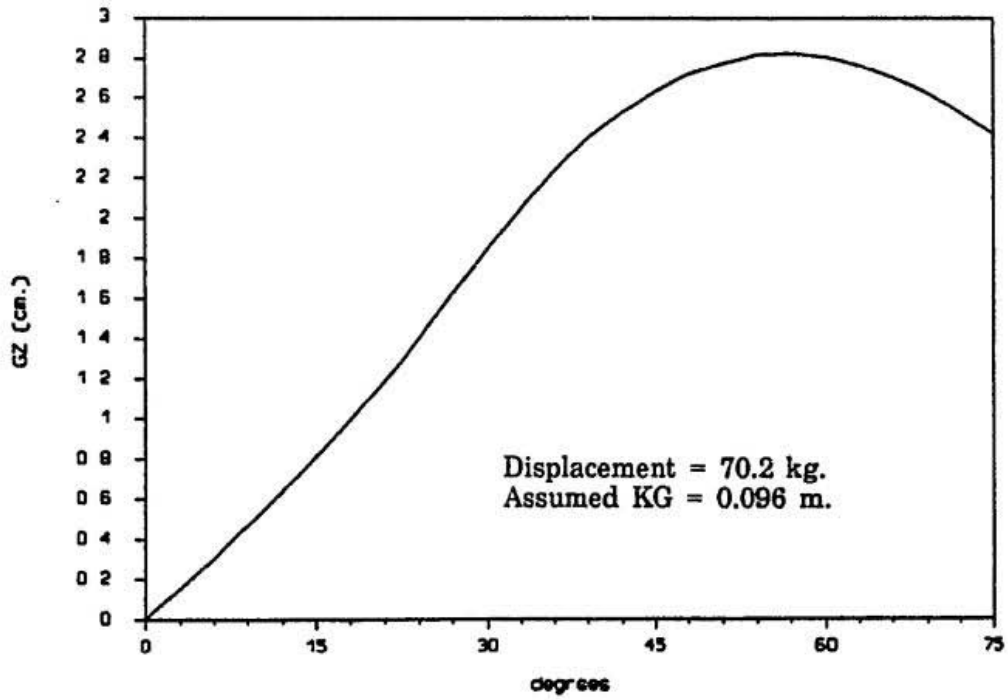

Figure 2.1.5.2
Restoring lever arm, GZ, curve for M.V. Arctic in first set of tests

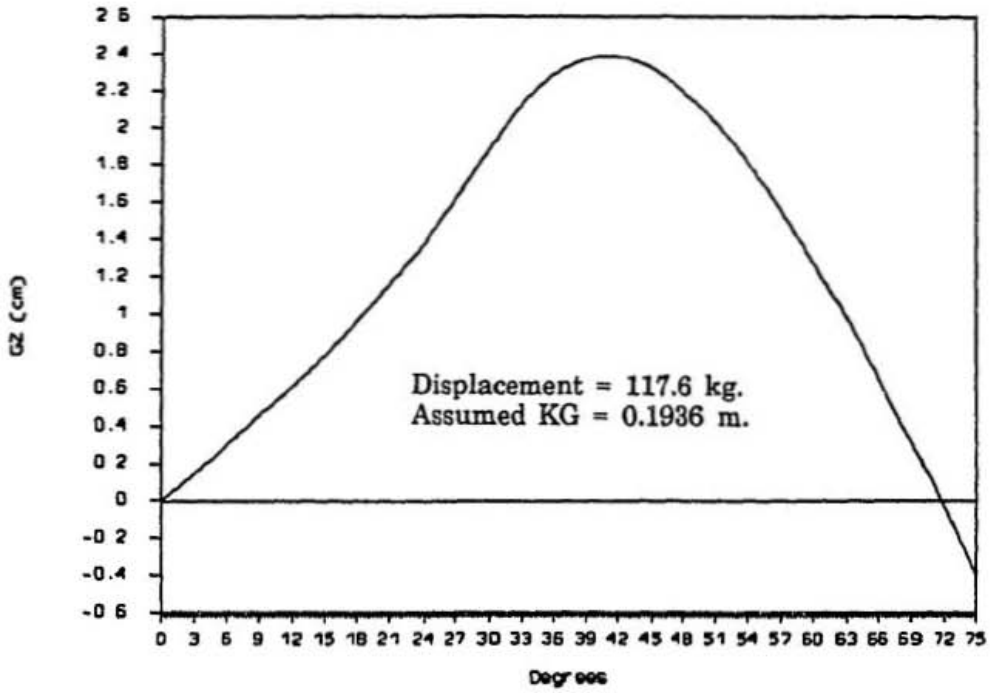

Figure 2.1.5.3
Restoring lever arm, GZ, curve for R-Class icebreaker in second set of tests

2.2 Data Collection

Two methods were used for collection of roll response data, the SELSPOT (SELective SPOT recognition) System and an angular induction transducer affixed to the hull.

The first set of tests used the SELSPOT System exclusively. The second set of tests repeated each test for the SELSPOT System and for the angular induction transducer.

The SELSPOT System, manufactured by Selective Electronic Co. (SELCOM) of Sweden, is an optical electronic device capable of measuring the three dimensional position of up to 30 points as defined by Light Emitting Diodes (LED's).

The LED's are pulsed every 3.2 milliseconds which allows a maximum sampling rate of 312.5 frames per second. Two electronic cameras with photosensitive detectors provide a digitized output of the displacement of each LED from the origin of its focal plane. Using vector calculus, the x, y, and z coordinates of each LED can be determined using the surveyed position of each camera and the line vectors to the LED's. Theoretically the line vectors from both cameras should intersect at the

centroid of the LED positions but, due to imperfections in the optical lenses, random noise in the digitization of the signals and the errors involved in the initial surveying of the LED's and the cameras, this does not occur. To accommodate this, an orthogonal line between the two line vectors is calculated and the actual position of the centroid of the LED's is considered to be a point halfway between the points of intersection of the orthogonal line and the two line vectors. The distance between these points of intersection is then used as a measure of the error of the LED's position. To minimize this error, the cameras should be placed as close as possible to 90 degrees from one another with respect to the object being measured.

Using at least 3 nonlinear LED's, the translational and rotational (six degrees of freedom) motion response of a rigid body can be measured as a function of time using the system software.

The primary system hardware consisted of either 4 or 8 LED's mounted on the model, a LED control unit secured above the model, two cameras mounted 90 degrees apart and an administration unit.

The initial x, y and z co-ordinates, in the tank co-ordinate system, of the LED's and the cameras are calculated using azimuth and inclination

measured with a transit. The same initial positions are then measured with the SELSPOT system.

Using this data, the system software calculates two transformation matrices (one for each camera) enabling measurements made by the cameras to be transformed to the tank co-ordinate system. To minimize error, a least squares routine is used in the transformation of the camera measurements to the tank co-ordinate system. The difference between the co-ordinates as measured by the transit and the rotated and translated camera co-ordinates is used as a measure of error.

The SELSPOT System will give accuracies of 0.2 cm in translation and 0.2 degrees in rotation.

The angular induction transducer was affixed directly to the model with its axis of rotation in the centreplane of the model, parallel to the waterline and containing the centre of gravity of the model. Its signal was recorded, along with the signal from the heave post potentiometer and the wave probes, on an HP3968A Instrumentation Tape Recorder. This is an 8 channel, 6 speed recorder capable of FM recording over a bandwidth of DC to 5 kHz and for direct recording of signals up to 64 kHz. Calibration of the heave post and angular induction transducer was performed

intermittently throughout the tests but it was found, as had been suggested, that the calibration did not vary.

The wave profiles generated for both sets of tests were recorded using two standard twin wire linear resistance wave probes. One was positioned 9.4 metres upstream of the centre of gravity of the model. The other, serving as a phase indicator, was placed 1 metre away from the model's centre of gravity and the same distance from the waveboard as the model.

As the resistance wave probes were temperature dependent, the wave generator was run for approximately 10 minutes to eliminate any water temperature gradients before calibration of the probes. Both probes were calibrated by raising and lowering the probe 5 cm from its zero point in increments of 1 cm. The voltage across the wires was measured at each increment. A linear regression was performed on the resultant data to determine the calibration coefficients. The calibration coefficients did not vary significantly from day to day.

The wave probe signals for both sets of tests were recorded on an HP3968A Instrumentation Tape Recorder. The signal was then digitized using a Keithley System 570 digitizer.

The Keithley System digitizer was also used to digitize the angular induction transducer's signal. Correspondence between the wave probe signal and the angular induction transducer's signal was achieved by recording them at the same time on the same tape and then digitizing them simultaneously through the Keithley System.

Correspondence between the SELSPOT data and the wave probe data was achieved by sending a trigger signal to the FM recorder when the SELSPOT system started recording data. This trigger signal was used to start the digitization of data in the Keithley System.

The SELSPOT data was converted to an appropriate form and stored on floppy diskettes after each test. Due to data storage constraints, the maximum scan rate of 312.5 samples/sec. was reduced by a factor of 4 to 78.1 samples/sec. In order to reduce the effect of noise, filtering, as discussed by Laurich [27], was performed by averaging several consecutive frames. In the first set of tests, this further reduced the sample rate to 9.75 samples/sec. for the M.V. Arctic tests and 19.5 samples/sec. for the R-Class tests. In the second set of tests, this reduced the sample rate for the R-Class icebreaker to 39 samples/sec. The angular induction transducer signal was digitized to 39 samples/sec. to correspond to this.

2.3 Reliability

In order to determine the repeatability or reliability of the tests, confidence intervals using the linearized damping coefficients were calculated. The linearized damping coefficients were used as this was the only way to ensure that the total damping was accounted for. There is a problem of energy sharing between the coefficients of the nonlinear damping forms. In other words, the coefficients of the nonlinear damping forms may vary but can give the same response when used in the rolling motion equation. The initial angles are within 4 degrees of each other for related tests which negates concerns about the variance of the initial angles influencing the linearized damping coefficients.

Due to the small size of the samples, the Student-t distribution was used. The assumption implicit in using the Student-t distribution is that the sample range is normally distributed. In order to investigate this, the range of the sample is divided evenly and the frequency of occurrence in each division is plotted in a histogram. If this resembles the bell shape of the normal distribution, i.e. its peak is in the middle, then the ogive is plotted. This is a graph of the cumulative frequency of occurrence versus the evenly divided range. For a normally distributed sample this has a

characteristic S curve. All the ogives for the tests had this characteristic curve. (See Fig. 2.3.1 to Fig. 2.3.3)

The mean and standard deviation of the linearized damping coefficients are then calculated. Using the Student-t method, 99% confidence intervals were calculated for related tests. This means that the probability of a damping coefficient being greater or less than the extreme values of this interval is 0.5%. All the tests considered for analysis fell within the appropriate confidence interval.

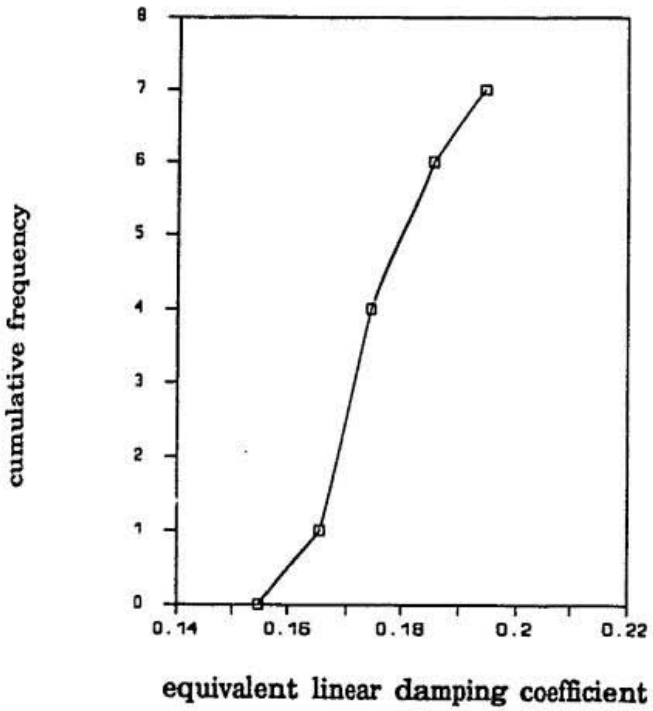

Figure 2.3.1
Ogive for R-Class icebreaker without bilge keels

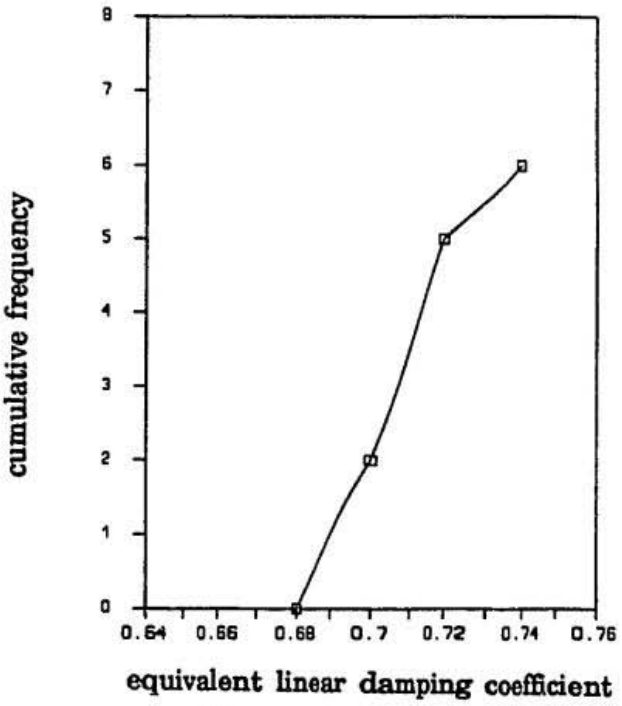

Figure 2.3.2
Ogive for R-Class icebreaker with bilge keels
1st moment of inertia

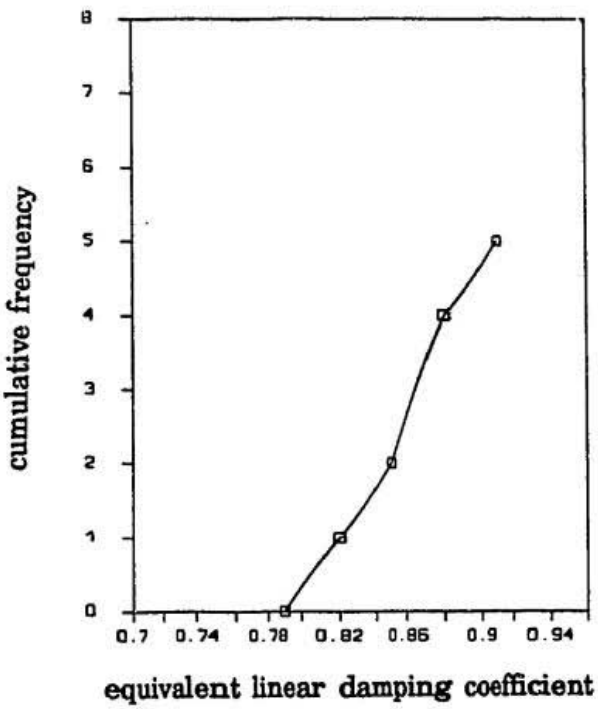

Figure 2.3.3
Ogive for R-Class icebreaker with bilge keels
2nd moment of inertia

3.0 METHODS OF ANALYSIS

Three methods of analyzing the roll decay were considered and compared; the Perturbation method, the Krylov-Bogoliubov technique or K.B. method, and the Energy method.

The first two techniques are accepted methods of analysis and can be considered the classical techniques. The Perturbation method assumes the nonlinear response as a small perturbation of the linear response. A perturbation series of the solution in a small perturbation parameter is substituted in the roll equation and solved numerically with the help of a least squares routine. The K.B. method uses the method of slowly varying parameters to find an equation for the rate of decay of the absolute value of the maxima and minima of the roll decay curve as a function of the damping moment parameters. Both these methods rely on the measurement and fitting of the damping moment form to the peak values of the roll decay curve.

The third method, the Energy method, is based on an energy approach as its name implies. With the help of a least squares routine, it uses the equivalence of the rate of change of the total energy of the system with the rate of energy dissipation in the damping to identify the damping

parameters. Unlike the previous two methods, this technique uses the whole curve in its analysis, not just the peak values. It also does not use the averaging technique and can handle a general form of the damping and restoring moments as well as being valid for large rolling motion.

3.1 The Perturbation Method

Perturbation methods assume that the nonlinear response of a ship is a small perturbation of the linear response. This means that the method is essentially valid for small nonlinearities only. Inherent in the solutions for this method is the assumption of small linear damping. The method is capable of handling only simple forms of the nonlinear damping moment, such as the linear plus quadratic and linear plus cubic velocity dependent forms, and linear restoring moments.

The Perturbation method for this analysis was taken from Mathisen and Price [9].

A general equation for ship rolling can be written in the form:

$$I\ddot{\phi} + B(\dot{\phi}) + C(\phi) = F \qquad 3.1.1$$

where ϕ = roll angle in radians
I = the mass moment of inertia in kg m^2 (dry structure plus fluid component)
$B(\dot{\phi})$ = the damping moment in Newton metres
$C(\phi)$ = the restoring moment in Newton metres
F = the exciting moment in Newton metres

For roll decay, F=0. Dividing the equation by the mass moment of inertia and choosing a linear plus quadratic form for the damping, the following equation is obtained:

$$\ddot{\phi} + d_1\dot{\phi} + \epsilon d_2\dot{\phi}|\dot{\phi}| + C(\phi) = 0 \qquad 3.1.2$$

where $C(\phi) = C\,\phi = \omega_n^2\,\phi$

A linear form was chosen for the restoring moment as the Perturbation method cannot handle a nonlinear form of restoring moment. All linear coefficients (d_1, ω_n^2) are assumed to be positive and the damping coefficients may be frequency dependent.

The Perturbation method assumes non-zero linear damping and small roll velocities. These assumptions provide that the nonlinear damping terms will have smaller magnitude than the linear damping terms. Given this, the small parameter $\epsilon, (0 < \epsilon < 1)$ is included for use in a perturbation expansion.

The perturbation expansion takes the form of a power series in the small parameter ϵ as follows:

$$\phi(t) = \phi_0(t) + \epsilon\phi_1(t) + \epsilon^2\phi_2(t) + \ldots \qquad 3.1.3$$

where t = time
ϕ_0 = basic solution
ϕ_1 = first order term
ϕ_2 = second order term.

The initial roll displacement is defined at time t=0.

The perturbation expansion is inserted into equation (3.1.2) and terms of the same order of magnitude of ϵ are sorted as follows:

$$\ddot{\phi}_0 + d_1\dot{\phi}_0 + C\phi_0 = 0 \qquad 3.1.4$$

$$\ddot{\phi}_1 + d_1\dot{\phi}_1 + C\phi_1 = -d_2\,\dot{\phi}_0^2\,\mathrm{sgn}(\dot{\phi}_0) \qquad 3.1.5$$

$$\ddot{\phi}_2 + d_1\dot{\phi}_2 + C\phi_2 = -d_2\,\dot{\phi}_0\,\dot{\phi}_1\,\mathrm{sgn}(\dot{\phi}_0 + \epsilon\dot{\phi}_1) \qquad 3.1.6$$

These equations may be solved to any order but for the purpose of simplicity they were restricted to second order. The right hand sides of the equations can be taken to be exciting terms defined by the lower order solutions.

The sgn (or sign) function is used to eliminate the need for the absolute value function in the quadratic damping term. It is defined as:

$$\mathrm{sgn}(\phi) = \begin{cases} +1 & \text{if } \phi > 0 \\ 0 & \text{if } \phi = 0 \\ -1 & \text{if } \phi < 0 \end{cases} \qquad 3.1.7$$

In deriving equations (3.1.4) to (3.1.6) only the order of the terms appropriate to the equation have been used in the sgn function.

Subcritical damping, i.e. $d_1^2 < 4C$ leads to the following solution for equation (3.1.4) :

$$\phi_0(t) = \Phi_{01}\, e^{\left(\frac{-d_1 t}{2}\right)} \cos(\omega_n t + \theta_{01}) \qquad 3.1.8$$

where Φ_{01} = initial amplitude of purely linear decay process, not the value of the first roll maximum or minimum

θ_{01} = phase angle. This is set to zero by choosing t=0 at the first maximum.

Differentiating equation (3.1.8) gives

$$\dot{\phi}_0 = \Phi_{01}\, e^{\left(\frac{-d_1 t}{2}\right)}[-0.5\, d_1 \cos(\omega_n t) - \omega_n \sin(\omega_n t)] \qquad 3.1.9$$

This equation can be simplified by the assumption that the linear damping coefficient is small compared with twice the natural frequency.

The simplified equation is as follows:

$$\dot{\phi}_0 \approx -\Phi_{01}\omega_n e^{(\frac{-d_1 t}{2})}\sin(\omega_n t) \qquad 3.1.10$$

Substituting equation (3.1.10) into equation (3.1.5), the right hand side is expanded into an odd Fourier series in the form

$$-d_2\dot{\phi}_0^2\,\mathrm{sgn}(\dot{\phi}_0) = d_2\Phi_{01}^2\omega_n^2 e^{(-d_1 t)}\sum_{p=1,3,\ldots}\frac{8\sin(p\omega_n t)}{\pi p(p+2)(p-2)} \qquad 3.1.11$$

Only the first harmonic of this Fourier series is considered, for two reasons: 1) the higher harmonics have small amplitude compared with the first harmonic; 2) the first harmonic occurs at the natural frequency of the system and the resultant resonant roll response will tend to filter out the higher frequency excitations.

As the analysis is taken to higher order terms, it can be seen that the amplitude terms of the solution form a geometric series whose summation gives

$$\phi(t) \approx \frac{3\pi d_1\Phi_{01}\cos(\omega_n t)}{3\pi d_1 e^{(\frac{d_1 t}{2})} - 8\epsilon d_2\Phi_{01}\omega_n} \qquad 3.1.12$$

The Perturbation method uses only the peak values of the roll decay record, R_i, $i = 1, 2, 3, \ldots$. In order to transform the time function (3.1.12) to accommodate R_i, the following is used:

$$t = \frac{i\pi}{\omega_n} \qquad i = 1, 2, 3, \ldots \qquad 3.1.13$$

Equation (3.1.12) then takes the form

$$R_i = \frac{3\pi d_1 \Phi_{01}}{3\pi d_1 e^{\left(\frac{d_1 \pi i}{2\omega_n}\right)} - 8\epsilon d_2 \Phi_{01} \omega_n} \qquad 3.1.14$$

The undamped natural frequency, ω_n, is taken as the mean frequency of the roll decay record. Mathisen and Price [9] state that the method may be inappropriate for analysis if there is any significant variation in the frequency.

As there are three unknowns, d_1, ϵd_2 and Φ_{01}, at least three maxima and minima must be available to provide estimates for these parameters. In order to minimize error, in practice a much larger number of maxima and minima are required together with a least squares routine. A suggested appropriate error term is the difference between the estimated peak value and the observed peak value. The sum of the squared error terms is referred to as the residual sum of squares, minimisation of which gives optimal estimates of the damping coefficients. However, this residual is a complicated non linear function of d_1 , ϵd_2 and Φ_{01} and may have a

number of local minima. It is possible to get negative values for the linear damping coefficient which is not considered to be realistic. Therefore, some form of constraining is required, with the constraint limiting the linear damping coefficient to positive values. After the parameters are estimated, they must be checked with the following convergence criterion for the geometric series.

$$\frac{8\epsilon d_2 \Phi_{01} \omega_n}{3\pi d_1} < 1 \quad , \quad t > 0 \qquad 3.1.15$$

If this is not satisfied, then the largest roll angle must be omitted from the analysis and the estimation repeated.

A computer programme was written using the above equations, (3.1.14) and (3.1.15) and a non linear least squares routine was used in order to analyze the simulated roll decay record generated for use in the comparison of the three techniques. The values of the nonlinear damping coefficients used in the simulated roll decay record were taken from the same paper, Mathisen and Price [9], as equations (3.1.14) and (3.1.15).

The nonlinear least squares routine required initial estimates of the three unknown parameters d_1, ϵd_2 and Φ_{01}. The routine turned out to be extremely sensitive to variations in the initial estimates. There was a very narrow range of values for each parameter, outside of which the routine

would not converge or would give unacceptable estimates. In fact, the initial estimates had to be so close to the actual values that there was often no need for the analysis to take place.

Additional disadvantages to the technique are its validity for small nonlinearities only, its assumption of small linear damping, and its dependence on large numbers of roll extrema, and therefore long roll decay records, for greater accuracy.

These disadvantages tend to negate the use of this method in the analysis of roll decay with bilge keels, as these records tend to have relatively few periods, large linear damping and large nonlinearities.

3.2 The Krylov-Bogoliubov Method (K.B. Method)

Sometimes called the averaging technique, this method uses the assumption of slowly varying parameters to derive an equation relating the rate of decay of the peak values to a polynomial function of the peak values having functions of the damping parameters as coefficients.

A general form of the roll equation, with an angle dependent and velocity dependent damping moment, can be written as

$$\ddot{\phi} + D(\phi) = -2\zeta\omega_n N(\phi, \dot{\phi}) \qquad 3.2.1$$

where $D(\phi)$ = restoring moment
$= \omega_n^2 \phi$ for K.B. method
ω_n = natural frequency of roll
ζ = linear damping ratio

and

$$N(\phi, \dot{\phi}) = 2\zeta\omega_n(\dot{\phi} + \epsilon_1|\phi|\dot{\phi} + \epsilon_2\phi^2\dot{\phi} + \epsilon_3|\dot{\phi}|\dot{\phi} + \epsilon_4\dot{\phi}^3) \qquad 3.2.2$$

The following relationships are assumed where $R = R(t)$ = maximum amplitude and $\theta = \theta(t)$ = phase angle and both are slowly varying.

i.e. $\frac{d^2R}{dt^2} \approx \frac{d^2\theta}{dt^2} \approx 0$

$$\phi = R\sin\psi \qquad 3.2.3$$

$$\dot{\phi} = \omega_n R\cos\psi \qquad 3.2.4$$

$$\psi = \omega_n t + \theta \qquad 3.2.5$$

Differentiating (3.2.3) gives

$$\dot{\phi} = \omega_n R\cos\psi + \dot{\theta}R\cos\psi + \dot{R}\sin\psi \qquad 3.2.6$$

Comparing (3.2.4) with (3.2.6) gives

$$\dot{R}\sin\psi + \dot{\theta}R\cos\psi = 0 \qquad 3.2.7$$

which leads to

$$\ddot{\phi} = \omega_n \dot{R}\cos\psi - \omega_n^2 R\sin\psi - \omega_n R\dot{\theta}\sin\psi \qquad 3.2.8$$

Substitution into (3.2.1) and using (3.2.7) gives

$$\dot{R}\omega_n\cos\psi - R\omega_n^2\sin\psi - \omega_n R\dot{\theta}\sin\psi + \omega_n^2 R\sin\psi = -2\zeta\omega_n N(R\sin\psi\ ,\ \omega_n R\cos\psi) \qquad 3.2.9$$

Multiplying (3.2.7) x $\omega_n\sin\psi$ and (3.2.9) x $\cos\psi$ and summing the results gives

$$\omega_n\dot{R}(\sin^2\psi + \cos^2\psi) = -2\zeta\omega_n N(R\sin\psi\ ,\ \omega_n R\cos\psi)\cos\psi \qquad 3.2.10$$

Since $\dot{R}$ is slowly varying, the right hand side of equation (3.2.9) becomes a slowly varying function of time and can be replaced with its average over a period. This leads to

$$\dot{R} = \frac{-1}{2\pi\omega_n}\int_0^{2\pi} 2\zeta\omega_n N(R\sin\psi\ ,\ \omega_n R\cos\psi)\cos\psi\, d\psi \qquad 3.2.11$$

The integration of the right hand side gives

$$\dot{R} = aR + bR^2 + cR^3 + \cdots \qquad 3.2.12$$

where

$$a = -\zeta \omega_n \qquad 3.2.13$$

$$b = \frac{-4}{3\pi} \zeta \omega_n (\epsilon_1 + 2\omega_n \epsilon_3) \qquad 3.2.14$$

$$c = \frac{-\zeta \omega_n}{4} (\epsilon_2 + 3\omega_n^2 \epsilon_4) \qquad 3.2.15$$

A least squares fit can be performed using roll decay data. In order to use a different form of the damping moment, the appropriate ϵ terms can be set to zero. For example, for the linear plus quadratic velocity dependent damping moment, ϵ_1 , ϵ_2 and ϵ_4 would be set to zero. Thus

$$\dot{R} = aR + bR^2 \qquad 3.2.16$$

where

$$a = -\zeta \omega_n \qquad 3.2.17$$

$$b = \frac{-8}{3\pi} \zeta \omega_n^2 \epsilon_3 \qquad 3.2.18$$

This was the form used in the analysis of the simulated roll decay record.

A computer programme was written incorporating equation (3.2.12) and allowing the appropriate term to be set to zero to tailor the nonlinear damping moment to the desired form.

As can be seen from the coefficients a, b and c in equations (3.2.12), (3.2.13) and (3.2.14), this technique does not wholly separate the influence of angle dependent and velocity dependent terms of the same order of magnitude.

As well, like the Perturbation method, only the peak values of the roll decay record are used. This means that long roll decay curves, which are often hard to obtain, are required to obtain sufficient peaks for a reasonably accurate fit. Care must also be taken when using the later, smaller amplitude part of the curve as these results are often inaccurate.

The K.B. method does not allow for a nonlinear restoring moment which makes its applicability to large angle motion analysis doubtful.

The advantages to this method lie in the fact that it is easy to apply (i.e. does not necessarily require a computer) and is relatively accurate for small damping moments and linear restoring moments.

3.3 The Energy Method

Although the concept behind the Energy method is not entirely new, its application to the analysis of ship rolling motion is novel. Bass and Haddara [7] present it as an alternative to the currently accepted methods.

This method uses the concept that the rate of change of the total energy in rolling motion is equivalent to the rate of change of energy dissipated by the roll damping.

The equation of rolling motion can be taken as:

$$\ddot{\phi} + D(\phi) = -2\zeta\omega_n N(\phi, \dot{\phi}) \qquad 3.3.1$$

where $D(\phi)$ can be nonlinear. Multiplying both sides by $\dot{\phi}$ gives

$$\frac{d}{dt}[\frac{1}{2}\dot{\phi}^2 + G(\phi)] = -2\zeta\omega_n N(\phi, \dot{\phi})\,\dot{\phi} \qquad 3.3.2$$

where

$$\frac{1}{2}\frac{d}{dt}(\dot{\phi}^2) = \dot{\phi}\,\ddot{\phi} \qquad 3.3.3$$

$$\frac{d}{dt}(G(\phi)) = D(\phi)\dot{\phi} \qquad 3.3.4$$

Integrating from t_i to t_{i+1} gives

$$H(t_i) - H(t_{i+1}) = 2\zeta\omega_n \int_{t_i}^{t_{i+1}} N(\phi, \dot{\phi})\,\dot{\phi}\,dt \qquad 3.3.5$$

where $H(t)$= the total energy of the ship per unit virtual moment of inertia at time t.

$$= \frac{1}{2}\dot{\phi}^2 + G(\phi) \qquad 3.3.6$$

Equation (3.3.5) shows the energy loss is equal to the energy dissipated in damping.

In order to apply the method to the analysis of roll damping, the roll decay curve is digitized at equally spaced instants in time. The number of points per period should be no less than 10 and need not be greater than 40. The roll velocity is calculated at each instant of time. Likewise the $H(t)$ term, equation (3.3.6), is evaluated at each instant. A parametric form for the roll damping moment is assumed and the integral on the right hand side of equation (3.3.5) is obtained numerically. The method of least squares is then used to obtain the coefficients of the damping moment.

If a general form of the roll damping moment is assumed as before

$$N(\phi,\dot{\phi}) = 2\zeta\omega_n[\dot{\phi} + \epsilon_1|\phi|\dot{\phi} + \epsilon_2\phi^2\dot{\phi} + \epsilon^3|\dot{\phi}|\dot{\phi} + \epsilon_4\dot{\phi}^3] \qquad 3.3.7$$

then let

$$\int_{t_i}^{t_{i+1}} N(\phi,\dot{\phi})\,\dot{\phi}\,dt = 2\zeta\omega_n \int_{t_i}^{t_{i+1}} [\dot{\phi}^2 + \epsilon_1|\phi|\dot{\phi}^2 + \epsilon_2\phi^2\dot{\phi}^2 + \epsilon_3|\dot{\phi}|\dot{\phi}^2 + \epsilon_4\dot{\phi}^4]\,dt \qquad 3.3.8$$

$$= \sum_{j=1}^{5} b_j n_{ij} \qquad 3.3.9$$

where

$$b_i = 2\,\zeta\,\omega_n\,\epsilon_i \qquad i = 1,2,3,4 \tag{3.3.10}$$

and

$$n_{i1} = \int_{t_i}^{t_{i+1}} \dot{\phi}^2(t)\,dt \tag{3.3.11}$$

$$n_{i2} = \int_{t_i}^{t_{i+1}} |\phi(t)|\dot{\phi}^2(t)\,dt \tag{3.3.12}$$

$$n_{i3} = \int_{t_i}^{t_{i+1}} \phi^2(t)\dot{\phi}^2(t)\,dt \tag{3.3.13}$$

$$n_{i4} = \int_{t_i}^{t_{i+1}} |\dot{\phi}(t)|\dot{\phi}^2(t)\,dt \tag{3.3.14}$$

$$n_{i5} = \int_{t_i}^{t_{i+1}} \dot{\phi}^4(t)\,dt \tag{3.3.15}$$

also let

$$Q_i(t) = H(t_i) - H(t_{i+1}) \tag{3.3.16}$$

Substituting into equation (3.3.9) gives

$$Q_i(t) = \sum_{j=1}^{5} b_j\,n_{ij} \tag{3.3.17}$$

A least squares method can then be used to find the coefficients which makes the mean squares difference between the left hand side and the right hand side of equation (3.3.17) a minimum.

As can be seen from equations (3.3.11) to (3.3.15), independent values for each component of the roll damping moment can be evaluated using this method.

A computer programme was written for this method allowing a choice of any combination of the components of the roll damping moment form shown in equation (3.3.7).

It was found upon use of the method that the analysis using the Energy method must be applied over an integer number of cycles and must be applied from peak value to peak value. This is due to the uneven change in energy over the cycle. It was found that the greatest change in energy occurred over the first quarter of the cycle, levelled off and decreased again, but not as abruptly, over the last half of the cycle. This uneven change in energy over the cycle is brought about by the nonlinear damping moment. The plots of the energy throughout the cycle were obtained using equation (3.3.6) and the experimental data record. (see Figs. 3.3.1 - 3.3.3).

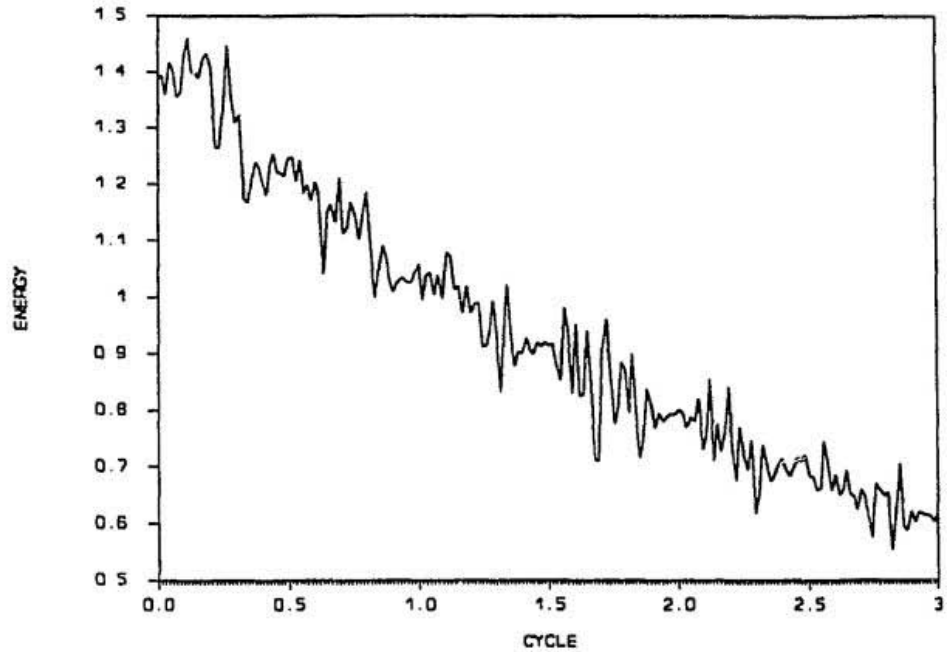

Figure 3.3.1
Energy change per cycle for tests without bilge keels

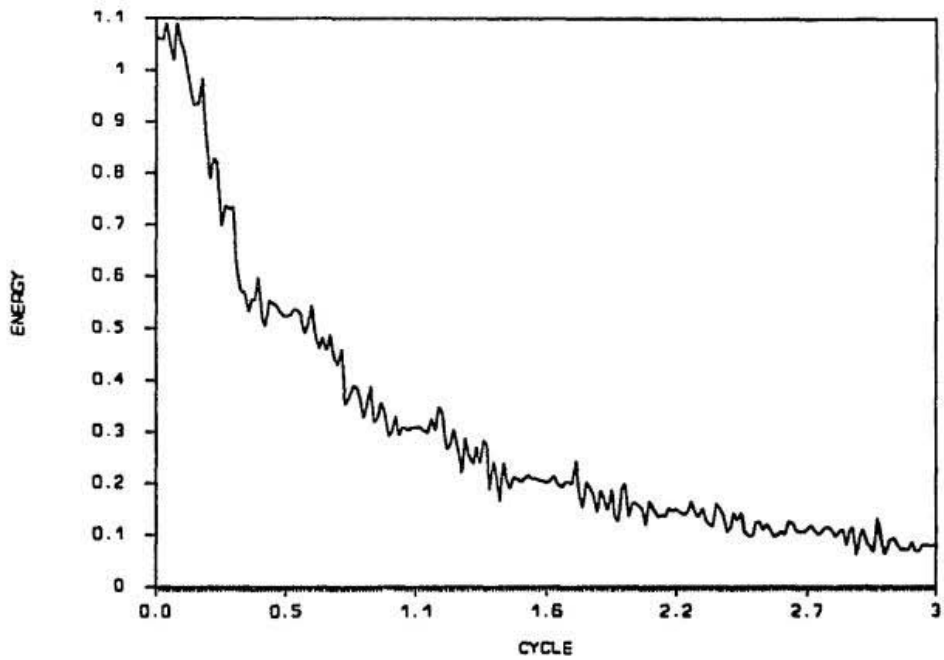

Figure 3.3.2
Energy change per cycle for tests with bilge keels and first moment of inertia

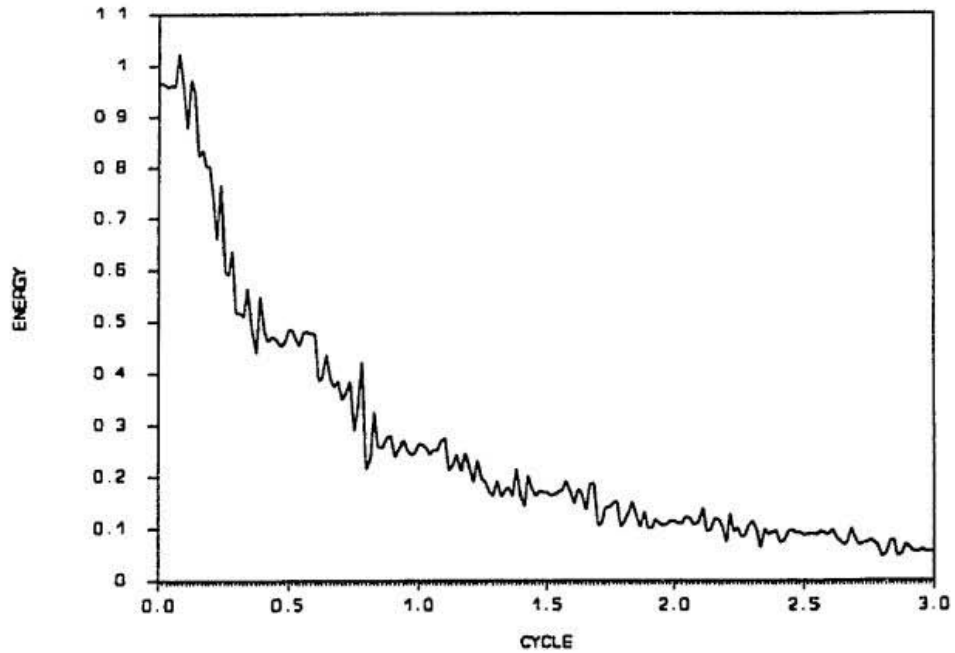

Figure 3.3.3
Energy change per cycle for tests with bilge keels and second moment of inertia

3.4 Comparison of Methods

In order to compare the three methods a simulated roll decay record was generated (see Fig. 3.4.1) using a Runge-Kutta routine and the following differential equation:

$$\ddot{\phi} + 2\zeta\omega_n\dot{\phi} + b\dot{\phi}|\dot{\phi}| + \omega_n^2\phi = 0 \qquad 3.4.1$$

The damping coefficients were taken to be $2\zeta\omega_n = 0.07$ $b = 0.5$ and the natural frequency $\omega_n = 3.14$

The damping coefficients obtained from the analyses by the three different methods were used to predict the peak values of the record and the results were compared (see Figs. 3.4.2 to 3.4.6). Initially, the decay record was predicted by substituting the estimated damping coefficients in the differential equation used in the Runge-Kutta routine. This method was not satisfactory as the Runge-Kutta routine had a cumulative effect on any errors in the damping coefficient estimation. Therefore, the following equation predicting the peak values of the record given the initial peak value was derived from the K.B. method and used, Marshfield [10].

$$R(t) = [\frac{e^{\zeta\omega_n t}}{C} - K]^{-1} \qquad C = \frac{\phi_0}{1 + K\phi_0} \qquad K = \frac{4b}{3\pi\zeta} \qquad 3.4.2$$

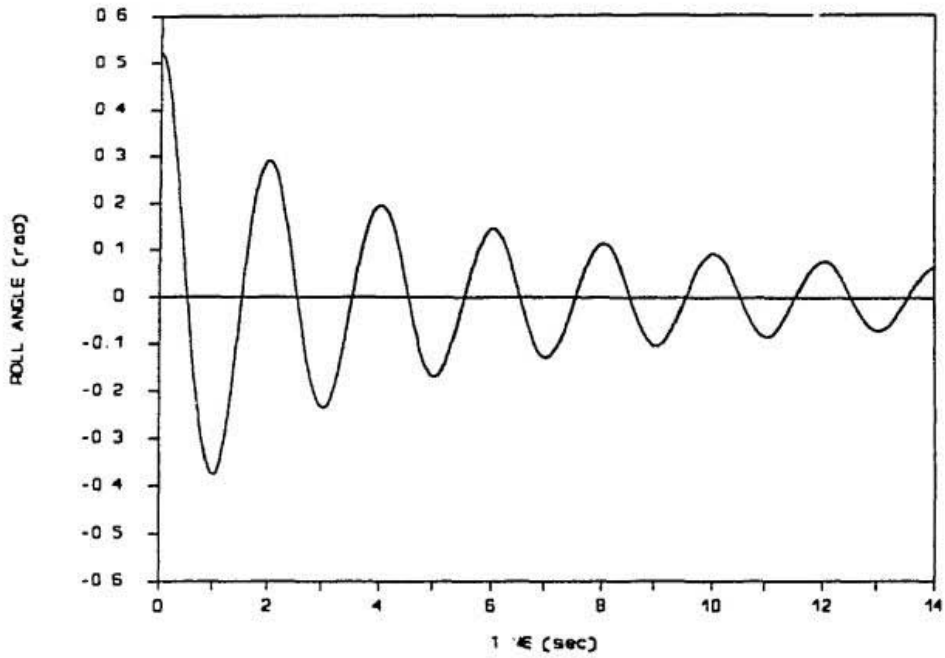

Figure 3.4.1
Simulated roll decay curve for use in comparing analysis methods

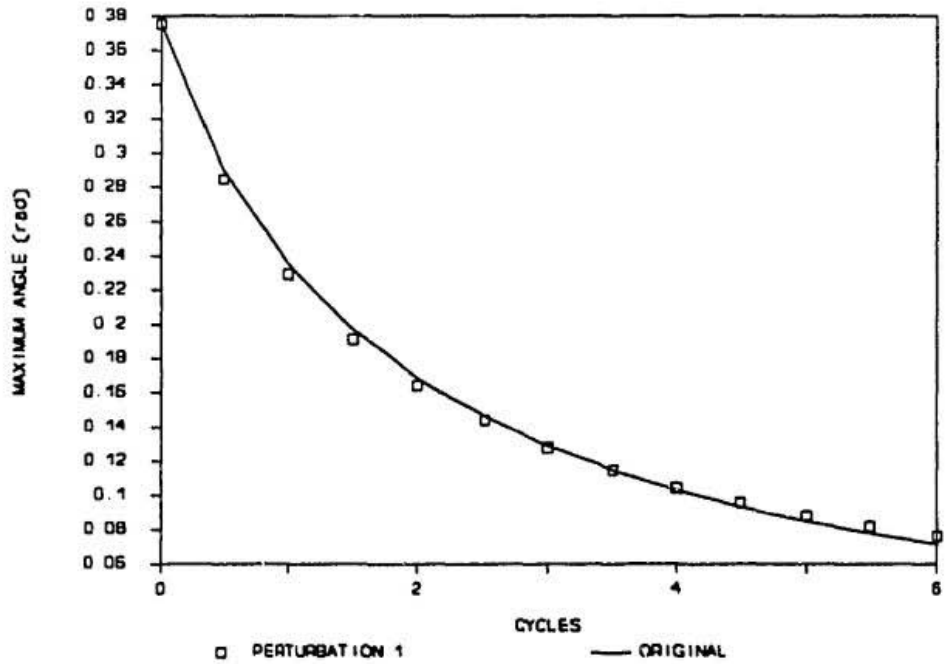

Figure 3.4.2
Prediction of simulated roll decay curve by Perturbation method, 1st. try, (approximate coefficient initial values)

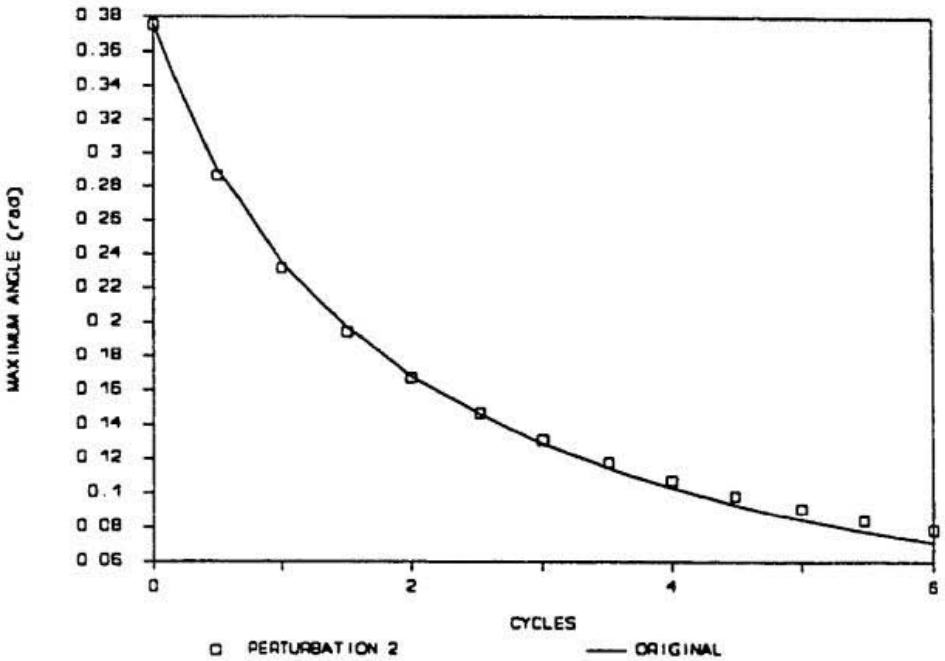

Figure 3.4.3
Prediction of simulated roll decay curve by Perturbation method, 2nd. try, (approximate coefficient initial values)

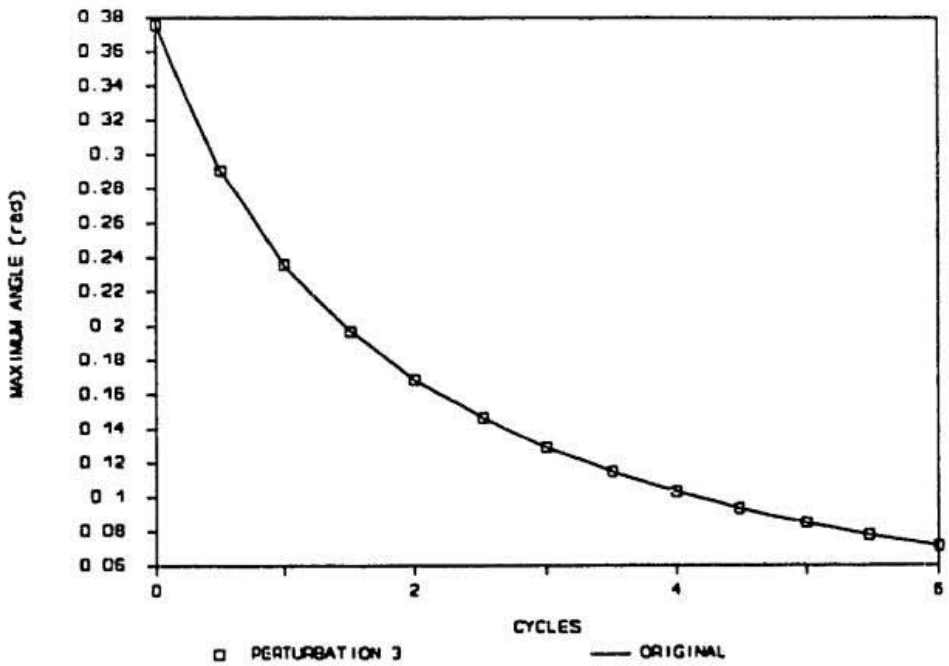

Figure 3.4.4
Prediction of simulated roll decay curve by Perturbation method, 3rd. try, (exact coefficient initial values)

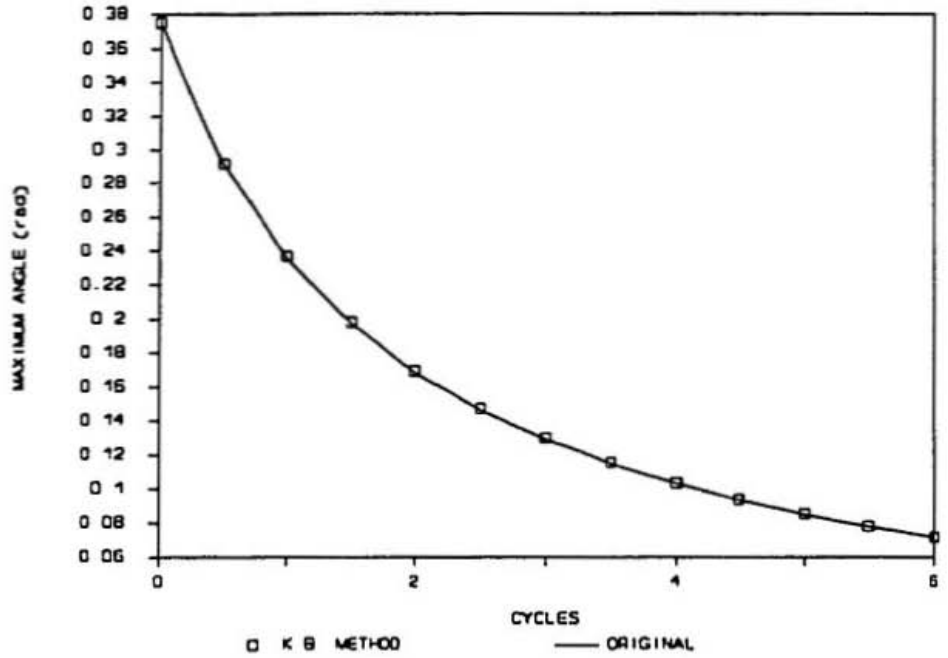

Figure 3.4.5
Prediction of simulated roll decay curve by Krylov-Bogoliubov method

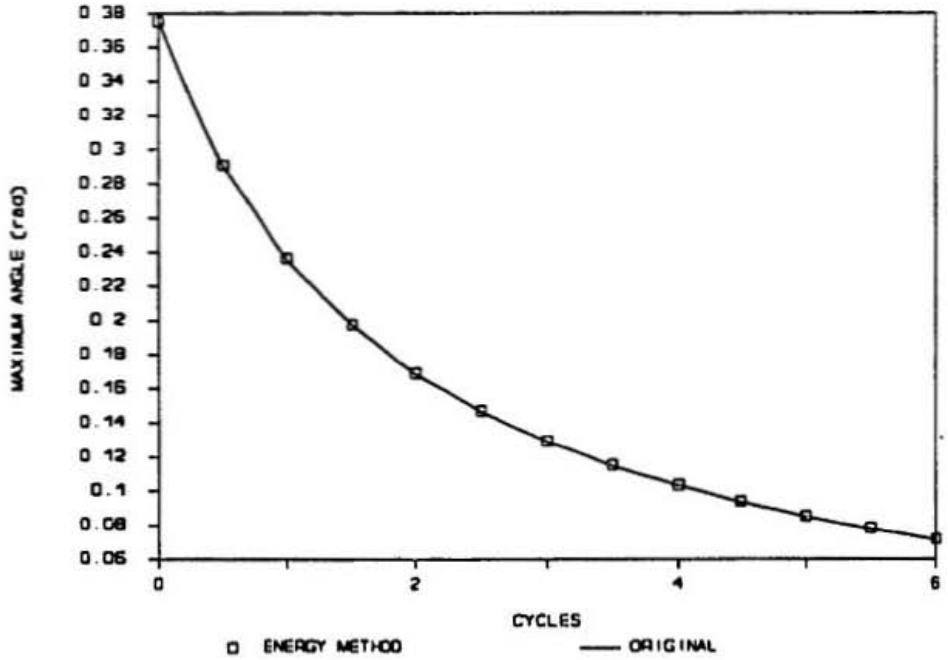

Figure 3.4.6
Prediction of simulated roll decay curve by Energy method

As can be seen from Figs. 3.4.2 to 3.4.6, the Energy method and the K.B. method estimates both provide very good predictions of the roll decay curve, with the Energy method having a marginally better percent error than the K.B. method. The difference between the K.B. and Energy methods would be clearer when applied to a case with nonlinear restoration as the K.B. method usually gives good results with linear restoration. However, the prediction equation was derived from the K.B. method and therefore required a linear restoration term. The Perturbation method's estimates gave reasonably good predictions, but only when the initial estimates of the damping coefficients were within one to two percent of the actual values. It was also difficult to arrive at an initial estimate of Φ_{01}, the purely linear decay process initial amplitude. In fact, the initial amplitude of the roll decay record was used.

From these comparisons it was determined that the Perturbation method was the least favored of the three methods. This was due to the need to know initial estimates of the damping coefficients, the narrow range within which the initial estimates had to lie, the inability to handle nonlinear restoring moments and its inapplicability for certain types of rolling motion, i.e. large nonlinearities and large amplitude motion. It also required the use of the roll decay peaks only, which necessitates the use relatively long roll decay records to obtain a reasonably accurate estimate.

Although the K.B. method uses roll peaks for its analysis, unlike the Perturbation method it is easy to apply, requires no initial estimates and resulted in a more accurate prediction than the Perturbation method. However, it does not allow for the use of a nonlinear restoring moment which tends to reduce its accuracy for large amplitude motion. It also cannot separate the influence of angle dependent and velocity dependent components of the same order of magnitude. Based on the comparison of the predictions and the versatility of the methods, this method was considered better than the Perturbation method but not as good as the Energy method.

The Energy method was considered the best of the three methods for three main reasons. Firstly, the method uses the whole roll decay record, not just the peak values. Thus shorter roll decay records can be used in the analysis. As well, the latter part of the roll decay record, with its attendant lower reliability, need not be used in the analysis. Secondly, the Energy method allows the use of a nonlinear restoring moment in the analysis. This provides a more accurate analysis of large amplitude motion. Thirdly, the influence of each component of the roll damping moment can be evaluated separately from the other components.

For these three reasons, and the fact that the Energy method coefficients resulted in predictions of the simulated roll decay as good as, or better than either of the other two methods, the Energy method was considered the best of the three methods.

4.0 ANALYSIS OF RESULTS

In this section, all analyses have been performed using the Energy Method. This was due to its favorable comparison with the other two methods and to its ability to analyze singular cases.

Six forms of the damping moment were used in each analysis. As the total number of possible combinations of the forms was too big to be feasible, the following forms were used to cover the accepted velocity and angle dependent forms.

1. Equivalent linear damping,

$$2\zeta\omega_n\dot{\phi} \qquad 4.0.1$$

2. Linear plus linear angle dependent damping,

$$2\zeta\omega_n\dot{\phi} + \epsilon_1|\phi|\dot{\phi} \qquad 4.0.2$$

3. Linear plus quadratic angle dependent damping,

$$2\zeta\omega_n\dot{\phi} + \epsilon_2\phi^2\dot{\phi} \qquad 4.0.3$$

4. Linear plus quadratic velocity dependent damping,

$$2\zeta\omega_n\dot{\phi} + \epsilon_3|\dot{\phi}|\dot{\phi} \qquad 4.0.4$$

5. Linear plus cubic velocity dependent damping,

$$2\zeta\omega_n\dot{\phi} + \epsilon_4\dot{\phi}^3 \qquad 4.0.5$$

6. A combination of all of the above.

$$2\zeta\omega_n\dot{\phi} + \epsilon_1|\phi|\dot{\phi} + \epsilon_2\phi^2\dot{\phi} + \epsilon_3|\dot{\phi}|\dot{\phi} + \epsilon_4\dot{\phi}^3 \qquad 4.0.6$$

The data recorded with the SELSPOT were found to be fairly 'noisy', with high frequencies superimposed on the record. Even with the filtering as described by Laurich [27], there was still sufficient noise to interfere with the analysis. As the data recorded with the angular induction transducer provided a much smoother signal, these data were used as the primary source for the single cycle analysis. These data were the record of the roll decay tests performed on the R-Class icebreaker in the second set of tests. Reasonable results were obtained when analyzing the SELSPOT data over the whole record. However, when single cycles were examined, the analysis did not seem as accurate.

4.1 Analysis of Single Cycles of Stillwater Roll Decay

The equivalent linear damping coefficient for each cycle in each roll decay test in the second set of tests (R-Class icebreaker only) was determined and plotted as a function of the initial amplitude of the cycle.

As the roll decay tests with bilge keels had only 3 cycles suitable for analysis, the results of the analyses of each set were plotted on one graph. A linear regression was performed on the equivalent linear damping coefficient values and plotted alongside them (See Figs 4.1.1 and 4.1.2). The equivalent linear damping coefficients for the roll decay tests without bilge keels were also plotted collectively along with their linear regression analysis as a comparison (See Fig. 4.1.3). These figures show distinctly the equivalent linear damping coefficient as a non constant function of the roll angle. The slope of the linear regression analysis increases sharply with the addition of bilge keels and again with an increase in the natural frequency.

It is interesting to note that although the addition of bilge keels effected a decrease in the natural frequency (from an average of 3.555 rad/sec without bilge keels to 3.412 rad/sec with bilge keels, due to the added moment of inertia effect of the bilge keels on the water), the equivalent linear damping coefficient and the slope of the linear regression increased.

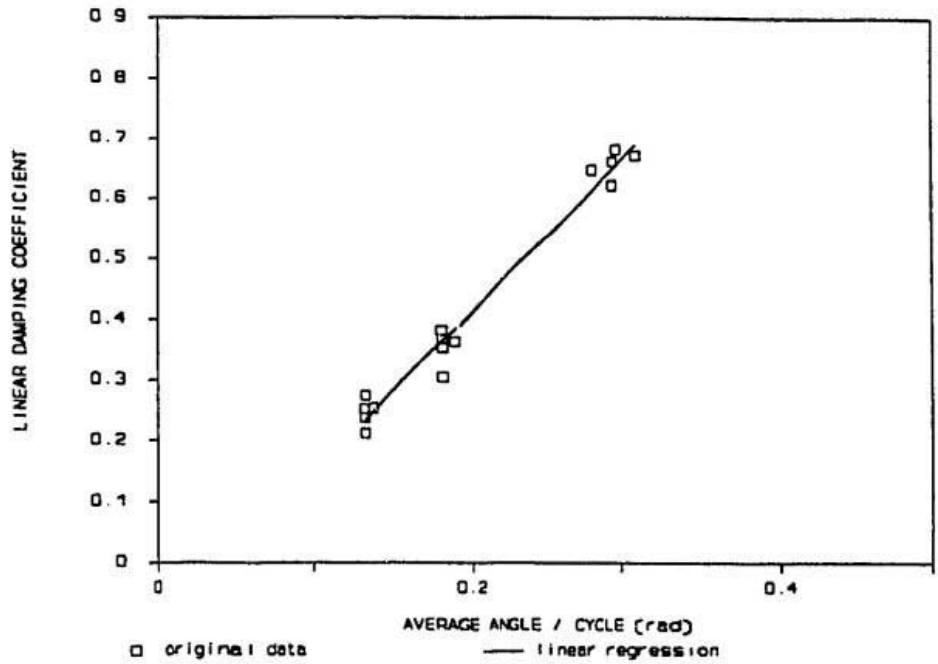

Figure 4.1.1
Collective linear damping for bilge keels (1st moment of inertia) and regression

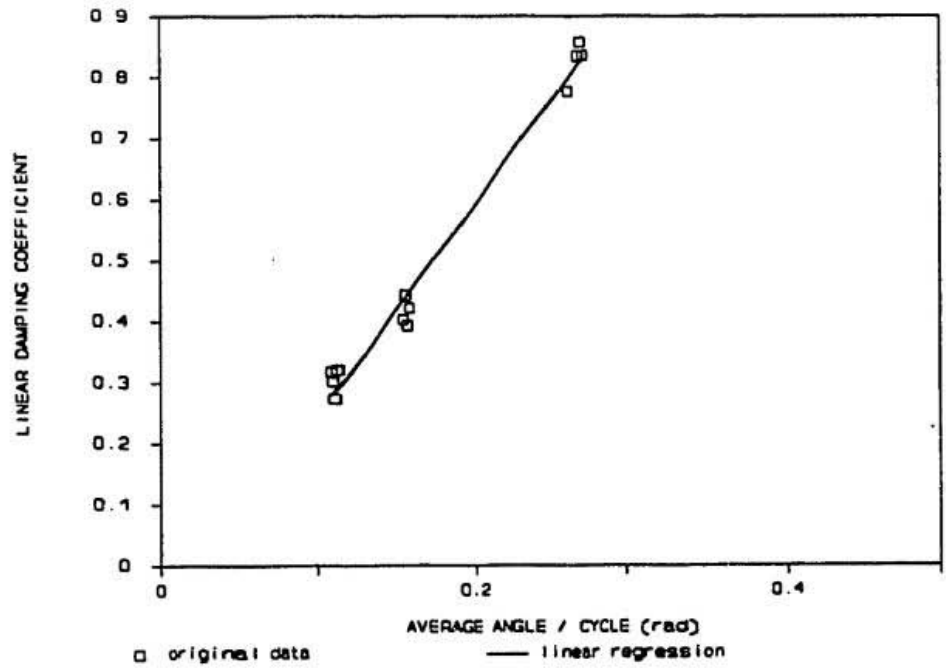

Figure 4.1.2
Collective linear damping for bilge keels (2nd moment of inertia) and regression

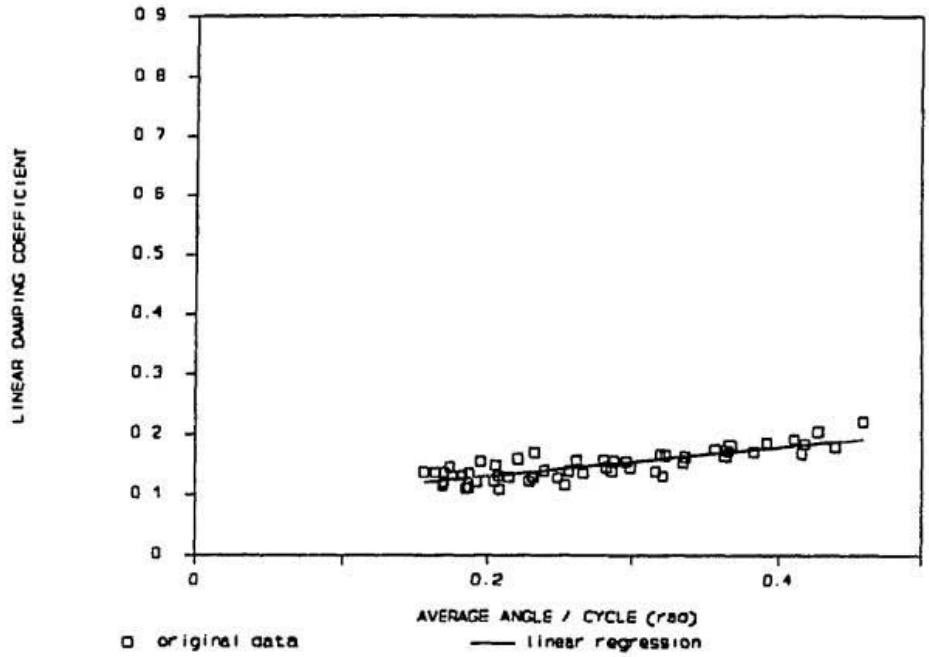

Figure 4.1.3
Collective linear damping for no bilge keels and regression

A decrease in the natural frequency would decrease the rate of dissipation of energy thus decreasing the equivalent linear damping. However, the addition of the bilge keels introduced more damping in the normal force damping, wave making damping and vortex shedding components. This increase in damping counteracts the decrease in equivalent linear damping due to the decrease in natural frequency and results in a net increase in the equivalent linear damping. The deliberate decrease in the dry mass moment of inertia produced by shifting the ballast weights closer to the centreline caused an increase in natural frequency and the expected increase in the equivalent linear damping as shown in Fig. 4.1.2..

Although the linear regression analyses performed on the collective per cycle equivalent linear damping coefficients seem to give a good fit, the equivalent linear damping coefficients for each cycle of the individual cases could indicate a more complex function of the roll angle. Figures 4.1.4 to 4.1.8 show the equivalent linear damping coefficients per cycle and the linear regression line plotted against the average angle of the cycle for five R-Class icebreaker stillwater roll tests.

In order to validate the single cycle analyses, damping coefficients of such an analysis were used to predict the peaks of the roll angles of the cycles preceding the chosen cycle. In order to predict these peaks, equation

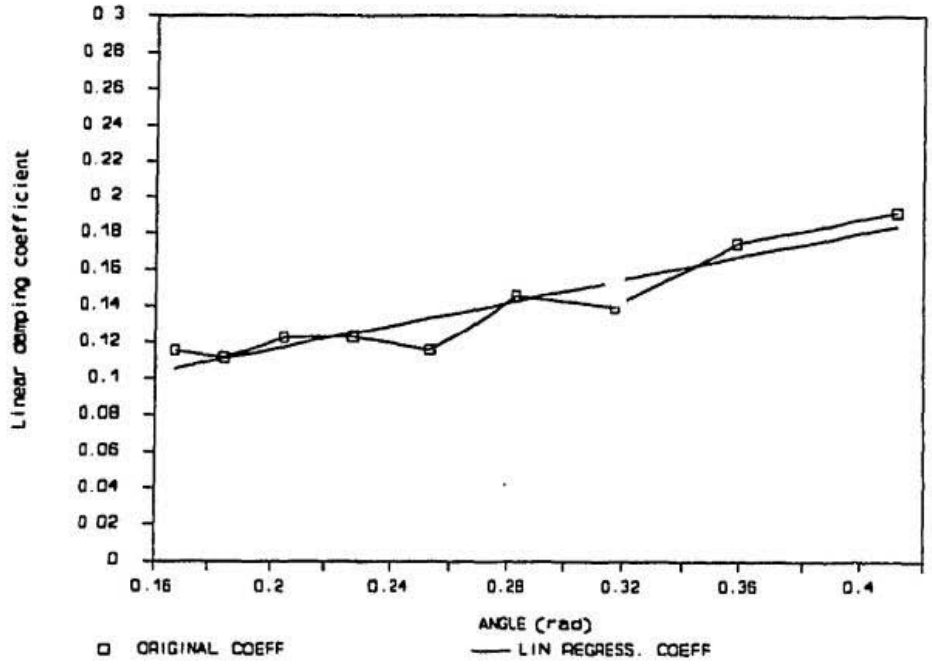

Figure 4.1.4
Individual linear damping per cycle for no bilge keels
Test 1

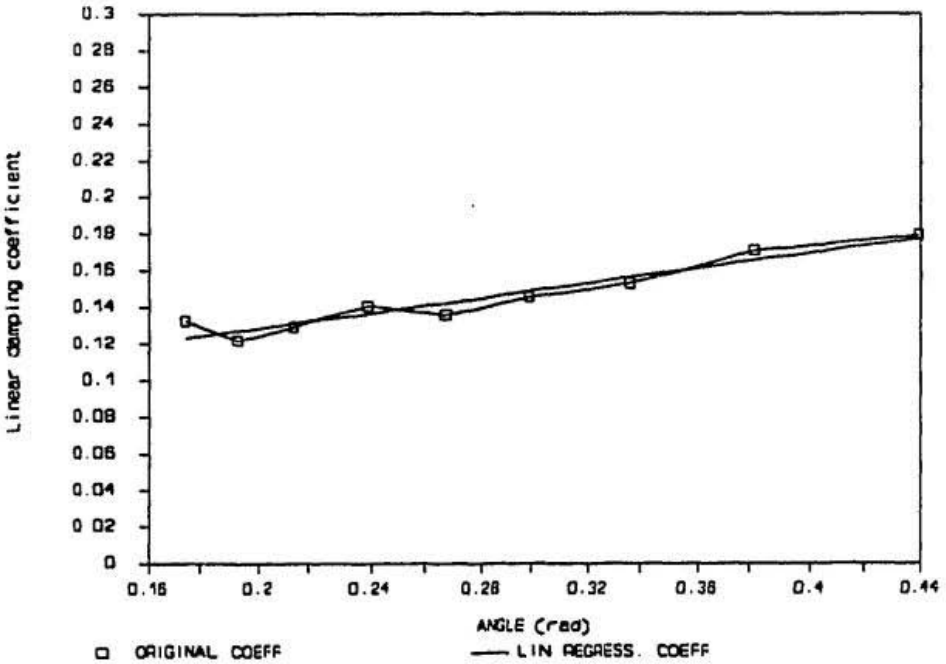

Figure 4.1.5
Individual linear damping per cycle for no bilge keels
Test 2

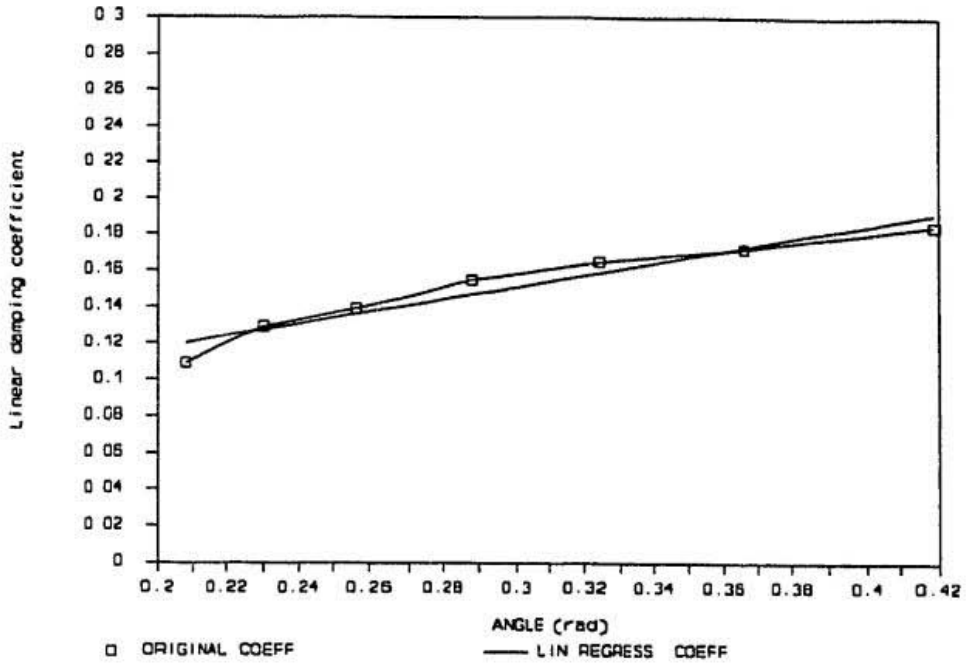

Figure 4.1.6
Individual linear damping per cycle for no bilge keels
Test 3

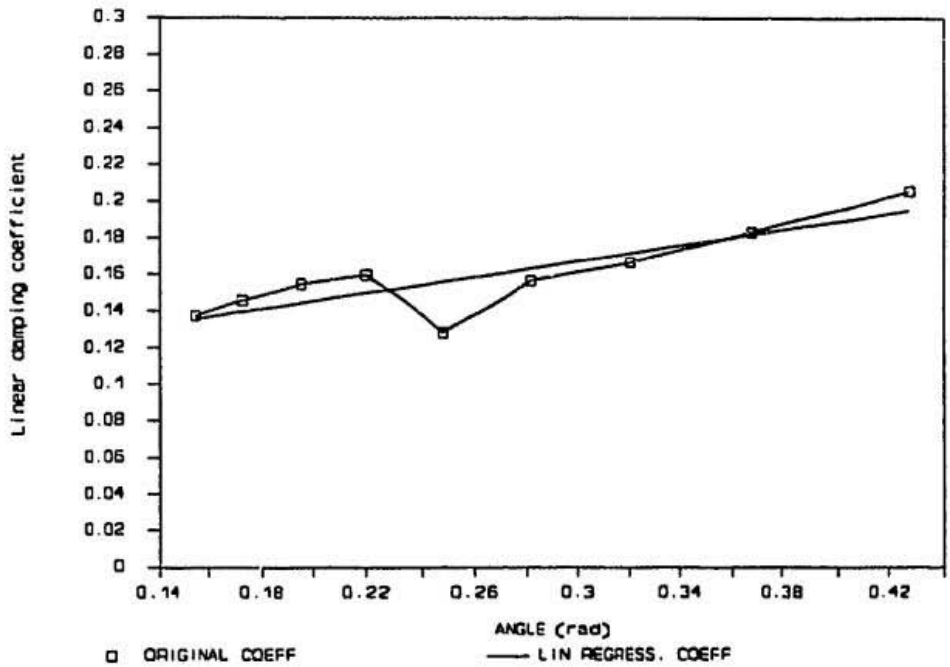

Figure 4.1.7
Individual linear damping per cycle for no bilge keels
Test 4

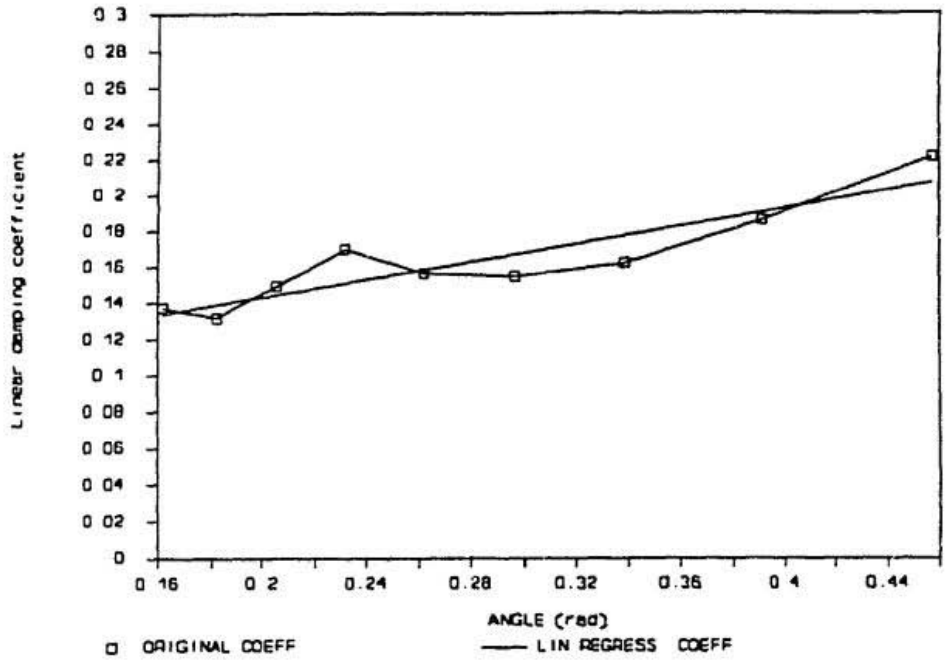

Figure 4.1.8
Individual linear damping per cycle for no bilge keels
Test 5

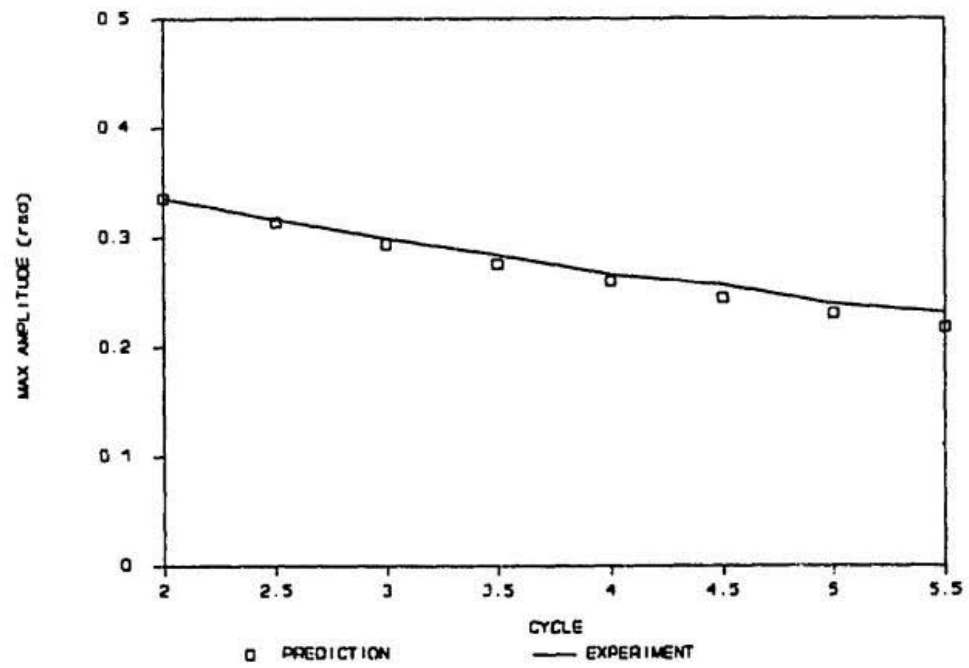

Figure 4.1.9
Prediction from single cycle starting one cycle outside the data range

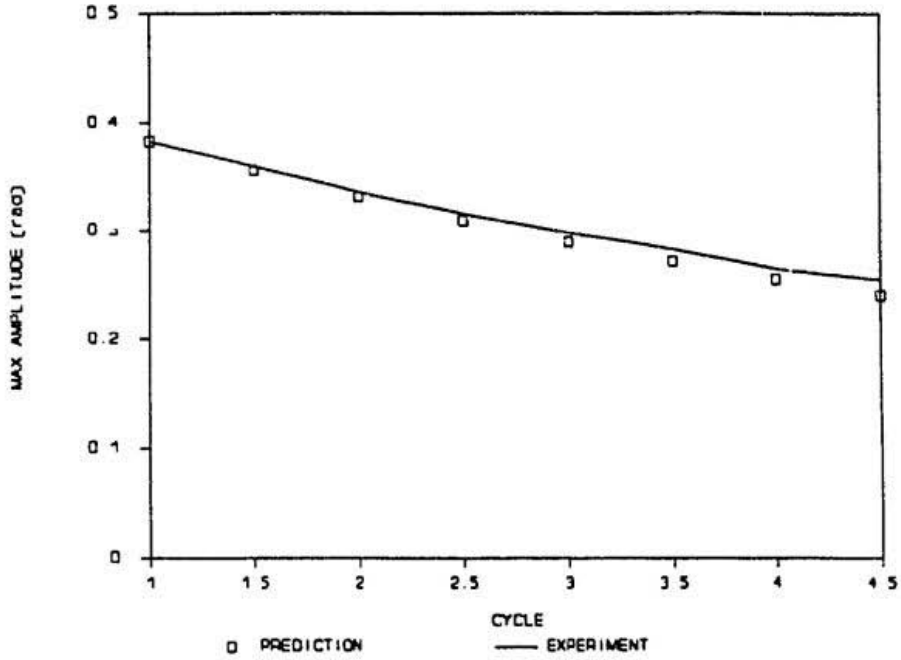

Figure 4.1.10
Prediction from single cycle starting two cycles outside the data range

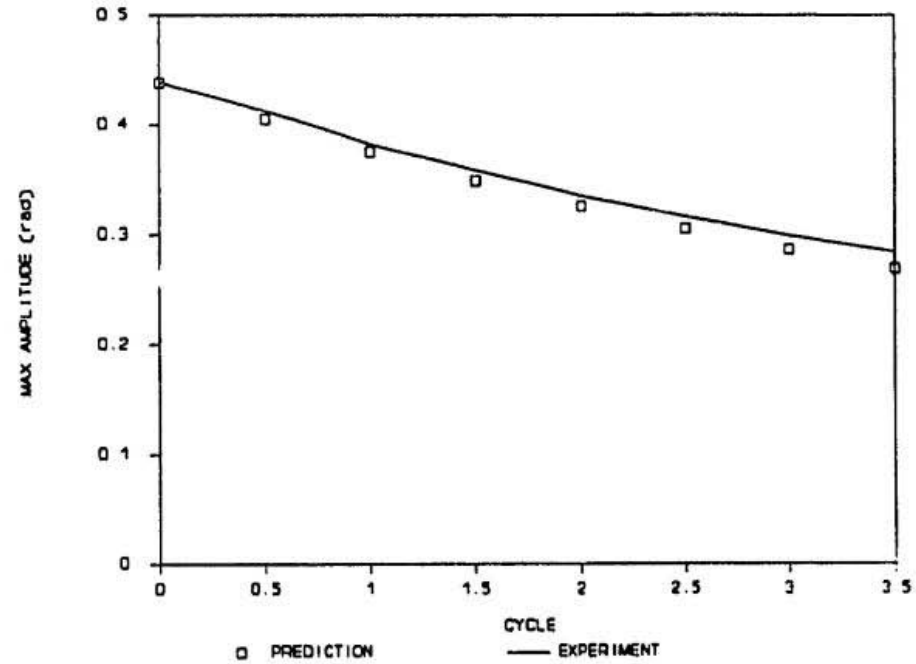

Figure 4.1.11
Prediction from single cycle starting three cycles outside the data range

(3.4.2) was used. The results of these predictions are shown in (Figs. 4.1.9-11). The predictions were made using the cubic velocity dependent form of the damping moment as these gave the best predictions. The linear angle dependent form gave approximately twice the error of the cubic velocity dependent form. This was still fairly good, being between 10% and 15% error at the worst case. The single cycle damping coefficients using the cubic velocity form gave very good predictions, within 5% error, up to 3 cycles outside the data range.

A qualitative look at the results of the Energy method single cycle analysis on the roll decay records of the R-Class icebreaker in the second set of tests is presented in Tables 4.1.1-8. If the coefficients of a damping term were negative in the analysis, this damping term was discarded as being physically unrealistic. The damping moment should always have the same sign as the angular velocity. In Tables 4.1.1-8, a 'Y' means the coefficients of that particular form were positive and indicate a possible viable form for the damping moment.

As can be seen from Tables 4.1.1-8, the angle dependent terms are consistently more viable than the velocity dependent terms. This would indicate a strong angular dependence of the damping moment. The cubic velocity dependent term gave the best predictions, however, the velocity

TABLE 4.1.1

Qualitative presentation of single cycle damping coefficients for R-Class icebreaker tests without bilge keels
Test 1

Cycle	Damping coefficients: linear	velocity dependent: quadratic	velocity dependent: cubic	angle dependent: linear	angle dependent: quadratic
1	Y	-	Y	-	-
2	Y	-	-	Y	Y
3	Y	-	-	Y	Y
4	Y	-	Y	Y	Y
5	Y	-	-	-	Y
6	Y	-	-	-	Y
7	Y	-	-	Y	Y
8	Y	-	-	-	Y
9	Y	Y	Y	-	Y

TABLE 4.1.2

Qualitative presentation of single cycle damping coefficients for R-class icebreaker tests without bilge keels
Test 2

Cycle	Damping coefficients: linear	velocity dependent: quadratic	velocity dependent: cubic	angle dependent: linear	angle dependent: quadratic
1	Y	-	-	Y	Y
2	Y	-	-	Y	Y
3	Y	-	Y	-	-
4	Y	-	-	-	-
5	Y	-	-	Y	Y
6	Y	-	-	-	Y
7	Y	-	-	Y	Y
8	Y	-	-	Y	Y
9	Y	-	-	Y	Y

TABLE 4.1.3

Qualitative presentation of single cycle damping coefficients for R-class icebreaker tests without bilge keel
Test 3

Cycle	Damping coefficients: linear	velocity dependent: quadratic	velocity dependent: cubic	angle dependent: linear	angle dependent: quadratic
1	Y	Y	Y	-	Y
2	Y	-	-	Y	Y
3	Y	-	-	-	Y
4	Y	-	Y	Y	Y
5	Y	-	Y	-	-
6	Y	-	-	-	Y
7	Y	-	-	-	Y
8	Y	-	-	-	Y
9	Y	Y	-	-	-

TABLE 4.1.4

Qualitative presentation of single cycle damping coefficients for R-class icebreaker tests without bilge keels
Test 4

Cycle	Damping coefficients: linear	velocity dependent: quadratic	velocity dependent: cubic	angle dependent: linear	angle dependent: quadratic
1	Y	-	-	Y	Y
2	Y	-	Y	Y	Y
3	Y	-	-	-	-
4	Y	Y	Y	-	-
5	Y	-	-	-	Y
6	Y	Y	Y	-	-
7	Y	-	-	-	Y
8	Y	-	-	-	Y
9	Y	-	-	-	-

TABLE 4.1.5

Qualitative presentation of single cycle damping coefficients for R-class icebreaker tests with bilge keels
1st moment of inertia
Test 1

Cycle	Damping coefficients: linear	velocity dependent: quadratic	velocity dependent: cubic	angle dependent: linear	angle dependent: quadratic
1	Y	-	-	Y	-
2	Y	-	-	Y	Y
3	Y	-	-	Y	-

TABLE 4.1.6

Qualitative presentation of single cycle damping coefficients for R-class icebreaker tests with bilge keels
1st moment of inertia
Test 2

Cycle	Damping coefficients: linear	velocity dependent: quadratic	velocity dependent: cubic	angle dependent: linear	angle dependent: quadratic
1	Y	-	-	-	-
2	Y	-	-	-	Y
3	Y	-	-	Y	Y

TABLE 4.1.7

Qualitative presentation of single cycle damping coefficients for R-class icebreaker tests with bilge keels
2nd moment of inertia
Test 1

Damping coefficients

Cycle	linear	velocity dependent		angle dependent	
		quadratic	cubic	linear	quadratic
1	Y	Y	Y	Y	Y
2	Y	-	-	-	-
3	Y	-	-	-	Y

TABLE 4.1.8

Qualitative presentation of single cycle damping coefficients for R-class icebreaker tests with bilge keels
2nd moment of inertia
Test 2

Damping coefficients

Cycle	linear	velocity dependent		angle dependent	
		quadratic	cubic	linear	quadratic
1	Y	Y	Y	Y	Y
2	Y	-	-	-	-
3	Y	Y	-	Y	Y

dependent models are actually angle dependent models with a nonlinear relation as shown in the following equation.

$$\dot{\phi} \approx \sqrt{\omega_n^2 R^2 - \omega_n^2 \phi^2} \qquad 4.1.1$$

This indication of angular dependence is supported by the plots of the equivalent linear damping coefficient per cycle as a function of the average angle of the cycle (Figs. 4.1.1-8).

4.2 Analysis of Whole Stillwater Roll Decay Record

As with the analysis of the single cycles, the damping coefficients from an analysis of half the roll decay records were used to predict the peaks of the whole record; this was performed to validate the whole record analysis. Both the Energy method and the K.B. method were used and compared with each other. The results of these predictions and comparisons are presented in Figs. 4.2.1-9. The K.B. method was used to give quadratic and cubic velocity dependent forms only. The predictions of both methods were made using the coefficients derived from analyses of the first 4 cycles of the roll decay records without bilge keels and from the first 2 cycles of the roll decay records with bilge keels. For the roll decay records without bilge keels, 9 cycles were predicted. For the roll decay records with bilge keels, 3 cycles were predicted.

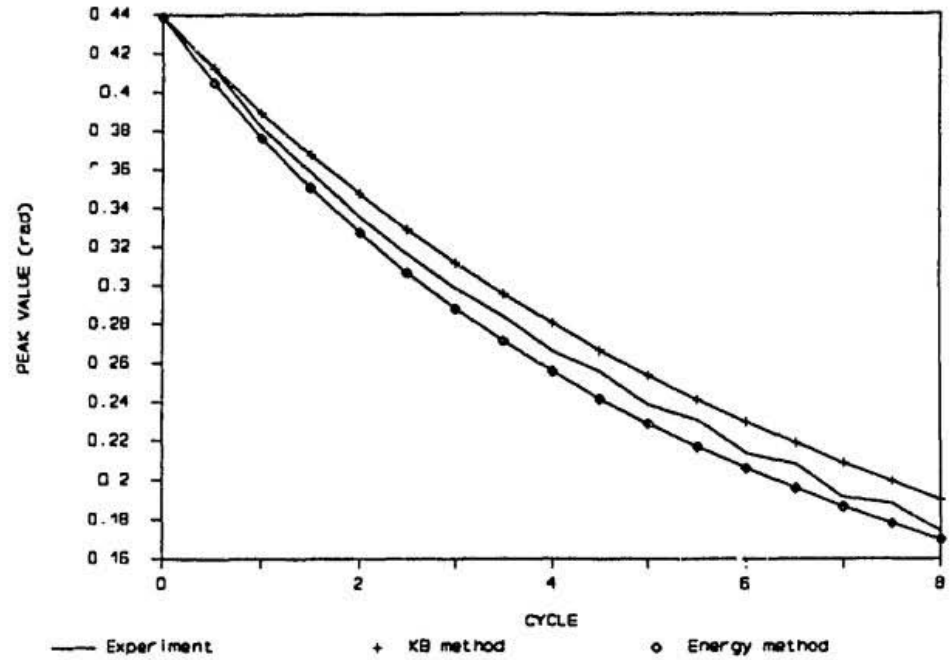

Figure 4.2.1

Predictions from half cycle to whole cycle using quadratic velocity component from K.B. method and Energy method for tests without bilge keels

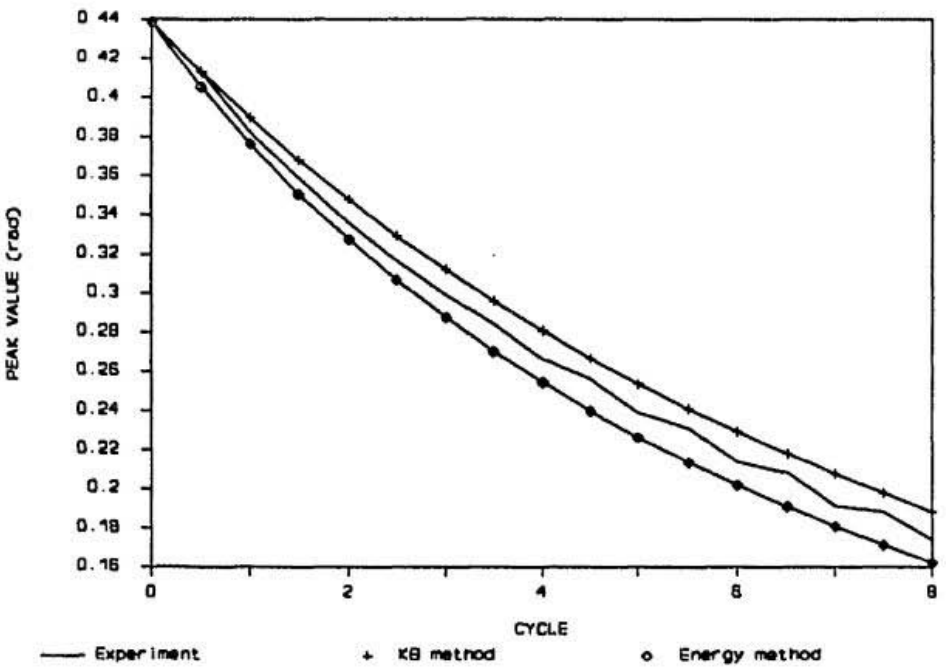

Figure 4.2.2

Predictions from half cycle to whole cycle using cubic velocity component from K.B. method and Energy method for tests without bilge keels

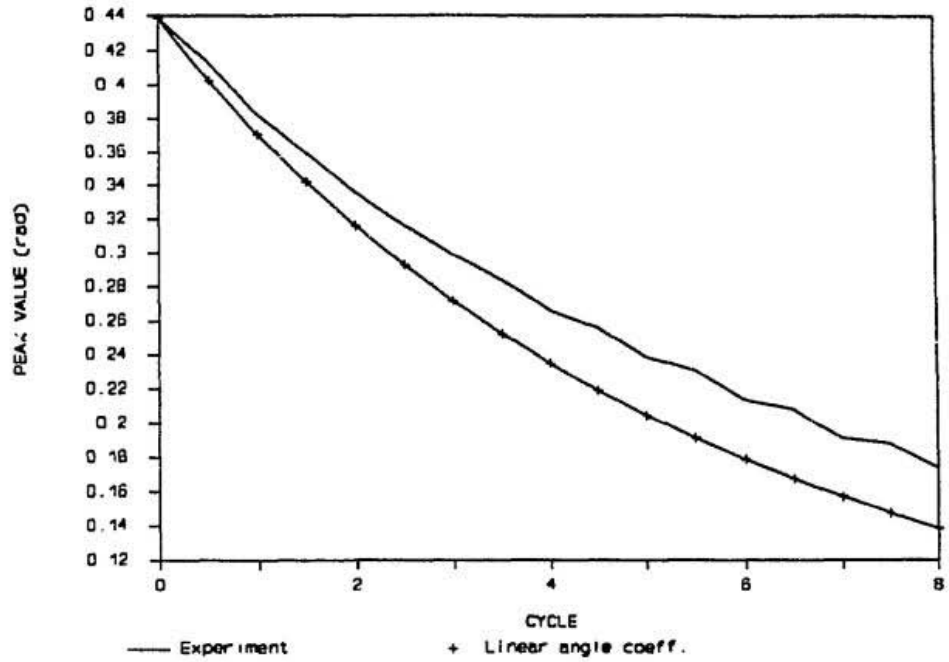

Figure 4.2.3
Predictions from half cycle to whole cycle using linear angle component from Energy method for tests without bilge keels

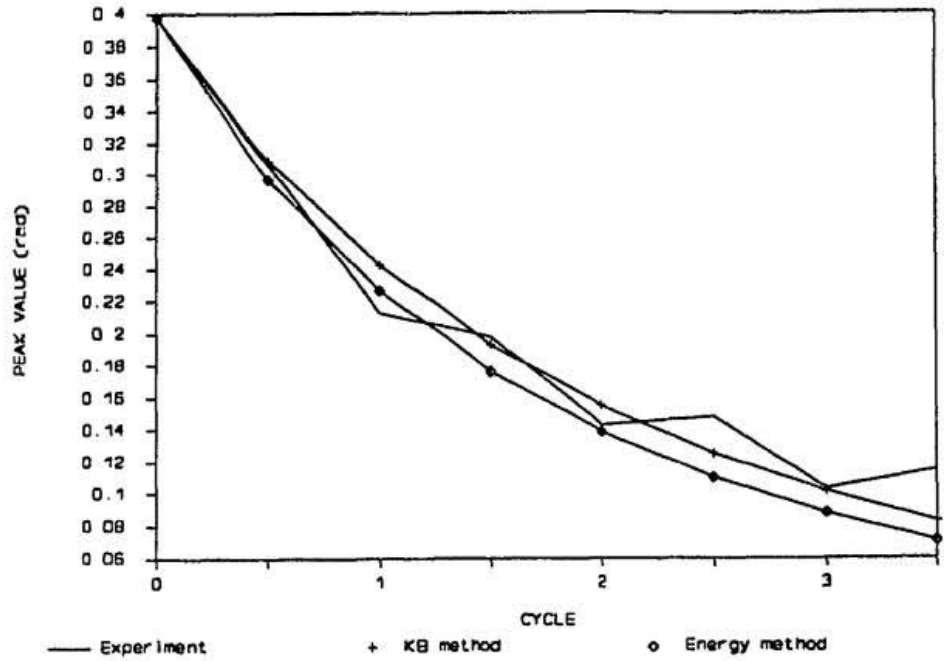

Figure 4.2.4

Predictions from half cycle to whole cycle using cubic velocity component from K.B. method and Energy method for tests with bilge keels and 1st. moment of inertia

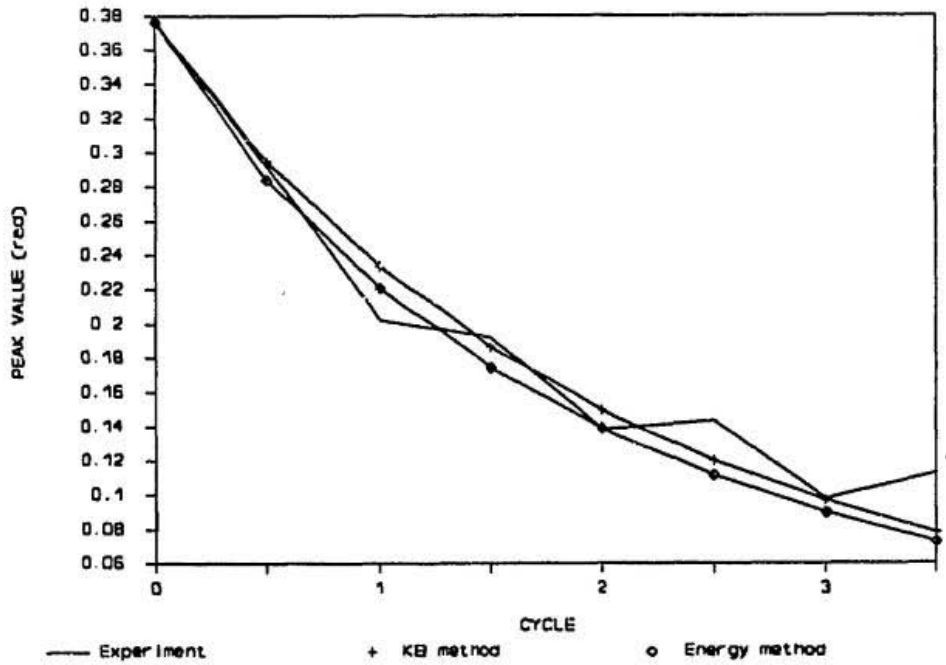

Figure 4.2.5

Predictions from half cycle to whole cycle using quadratic velocity component from K.B. method and Energy method for tests with bilge keels and 1st. moment of inertia

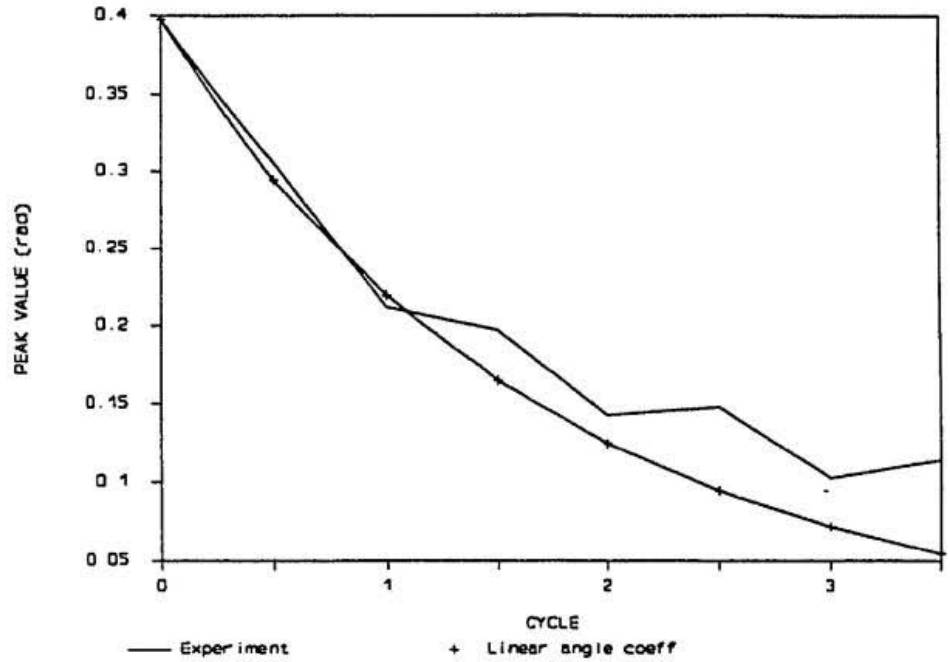

Figure 4.2.6
Predictions from half cycle to whole cycle using linear angle component from Energy method for tests with bilge keels and 1st. moment of inertia

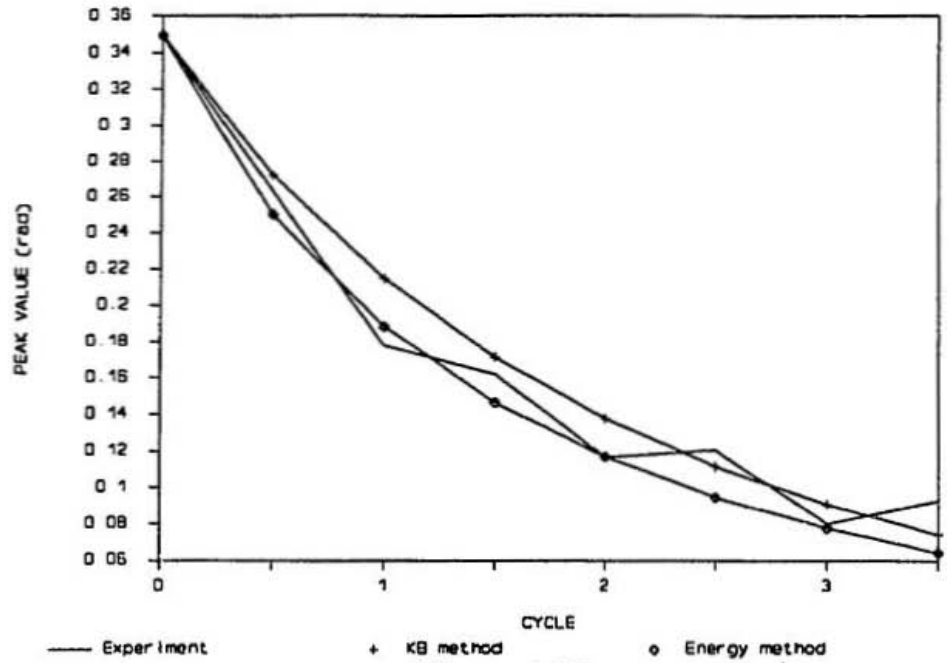

Figure 4.2.7

Predictions from half cycle to whole cycle using quadratic velocity component from K.B. method and Energy method for tests with bilge keels and 2nd. moment of inertia

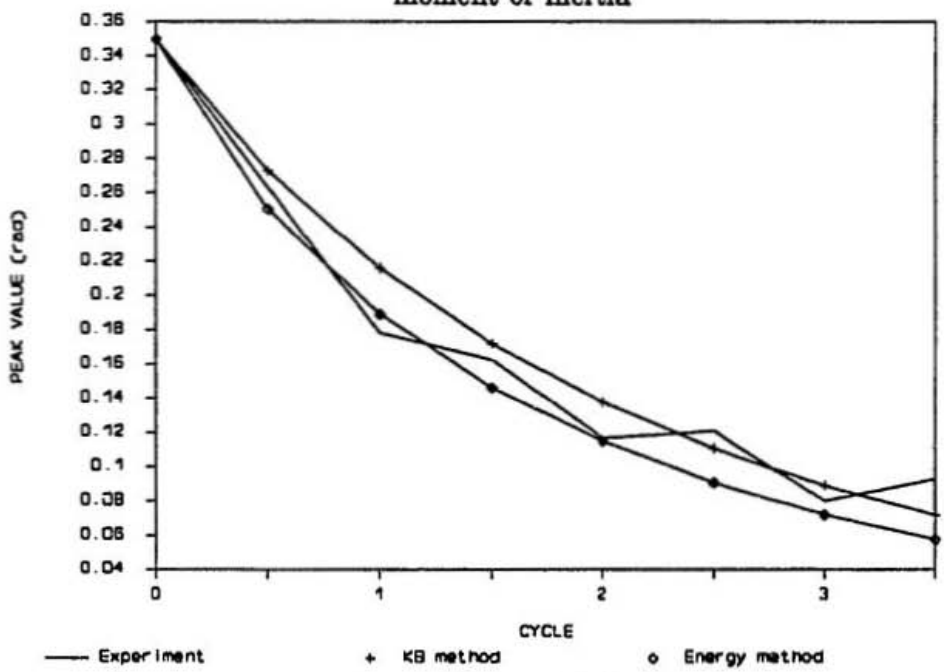

Figure 4.2.8

Predictions from half cycle to whole cycle using cubic velocity component from K.B. method and Energy method for tests with bilge keels and 2nd. moment of inertia

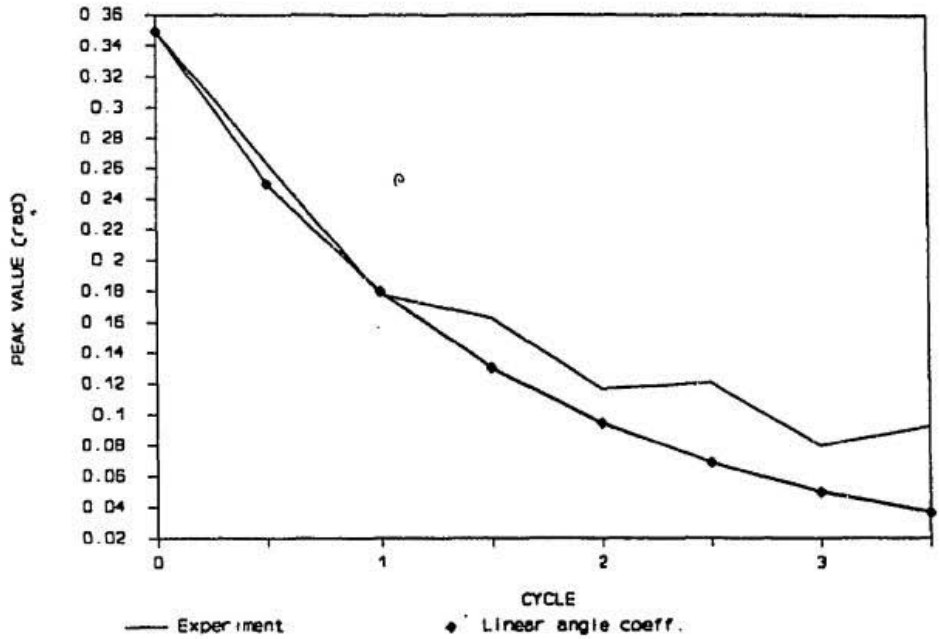

Figure 4.2.9
Predictions from half cycle to whole cycle using linear angle components from Energy method for tests with bilge keels and 2nd moment of inertia

Both the Energy method and the K.B. method gave good predictions for the roll decay records without bilge keels; within 8-10% error as the worst case for the K.B. method and within 4-6% error as the worst case for the Energy method using quadratic and cubic velocity dependent damping coefficient.

The K.B. method gave slightly better predictions of the roll decay records with bilge keels. This was surprising as the K.B. method used 5 peak values only for the analysis. In the tests with bilge keels, the damping was sufficiently high as to allow small angles of roll only and the GZ curve is quite linear over the range of these roll angles. This was to the advantage of the K.B. method which assumes a linear restoring moment. However, beyond the third cycle the Energy method gave better results. The roll decay records with bilge keels were more suspect than the records without bilge keels as there seemed to be some bias as well as some drift of the zero values of the record with time for the records with bilge keels. Attempts were made to offset these problems by various methods of zeroing and filtering but, in the end, as nothing seemed to alleviate the problem, the records were left as is in their raw data form. The problem can be seen in the curve of the peak values with time. Instead of following a smooth curve, the peak values decrease in a discontinuous manner giving a 'zig zag' appearance to the curve (See Figs. 4.2.4-9).

With the exception of the M. V. "Arctic" stillwater roll tests, the linear and quadratic angle dependent forms used in the analysis did not give as good predictions as the quadratic and cubic velocity dependent terms.

For the records of the R-Class icebreaker without bilge keels, the angle dependent terms gave predictions with errors less than 12 and 13% up to the latter part of the range outside the data used in the analysis (See Figs. 4.2.1-6). For the records of the M. V. "Arctic" without bilge keels, the predictions had errors of less than 6%. For the records of the R-Class icebreaker with bilge keels, the predictions using the angle dependent terms had errors ranging from 30-60%. The Energy method tended to overdamp the prediction. This can be explained by the fact that the first cycles of the roll decay record were used to calculate the damping coefficients. Figures 3.3.1-3 show that the first few cycles have large changes in energy indicating large damping. As this damping was used to predict the rest of the curve, it is understandable that the prediction was overdamped.

A qualitative look at the half record Energy method analyses of the aforementioned records is presented in Tables 4.2.1-3. As with the single cycle analyses, a negative coefficient was considered unrealistic. A 'Y' in the table indicates the coefficients of that form were positive and indicate a possible viable form for the damping moment.

The tests without bilge keels and the tests with bilge keels and the 2nd moment of inertia had viable terms for all the damping coefficients used in the analysis. The tests with bilge keels and the 1st moment of inertia showed little or no angle dependence. This is a puzzling result as the tests had a similar natural frequency to the tests without bilge keels which would indicate that the addition of the bilge keels produced less angle dependence in the damping moment. However, if this was the case, the tests with bilge keels and the 2nd moment of inertia would be expected to have less angle dependence in the damping moment. This is not the case. A possible explanation is that the drift in the zero values in the tests with bilge keels has affected the analysis.

The increase in the natural frequency due to the decrease in the mass moment of inertia resulted in an increase in the damping moment due to an increase in the number of roll cycles per minute. This increase in the

TABLE 4.2.1

Qualitative presentation of damping coefficients for whole roll decay test
R-Class icebreaker tests without bilge keels

	Damping coefficients				
Test	linear	velocity dependent		angle dependent	
		quadratic	cubic	linear	quadratic
Test 1	Y	Y	Y	Y	Y
Test 2	Y	Y	Y	Y	Y

TABLE 4.2.2

Qualitative presentation of damping coefficients for whole roll decay test
R-Class icebreaker tests with bilge keels,
1st moment of inertia

	Damping coefficients				
Test	linear	velocity dependent		angle dependent	
		quadratic	cubic	linear	quadratic
Test 1	Y	Y	Y	Y	-
Test 2	Y	Y	Y	-	-

TABLE 4.2.3

Qualitative presentation of damping coefficients for whole roll decay test
R-Class icebreaker tests with bilge keels,
2nd moment of inertia

	Damping coefficients				
Test	linear	velocity dependent		angle dependent	
		quadratic	cubic	linear	quadratic
Test 1	Y	Y	Y	Y	Y
Test 2	Y	Y	Y	Y	Y

number of cycles per minute increased the rate of energy dissipation which shows up as an increase in the damping moment. The roll decay equation

$$\ddot{\phi} + 2\zeta\omega_n N(\phi,\dot{\phi}) + C(\phi) = 0 \qquad 4.2.1$$

where ω_n = natural frequency.
ζ = linear damping ratio

would indicate a linear increase in the damping moment with an increase in the natural frequency assuming ζ and ϵ are not functions of the frequency. An increase in the equivalent linear damping moment due to an increase in the natural frequency is shown in the R-Class icebreaker roll decay records in the first and second sets of tests. Equation 4.2.1 would indicate that this increase in the equivalent linear damping moment would be linear. This is not necessarily shown in the experiment. The first set of tests show that a change in the average natural frequency of 4 % gives a 7 % change in the equivalent linear damping coefficient. The second set of tests show that a 9.2% change in the average natural frequency gives a 15.4% change in the equivalent linear damping moment. These results are not conclusive, however, as there are only two variations in either set of tests. Further tests with more variations would be required to come to any firmer idea of the form of the dependence of the roll damping moment on the natural frequency of roll.

The equivalent linear damping form is used in these comparisons in order to account for the total damping. Only two moments of inertia are used in the first set of tests as the series of roll decay tests with the intermediate moment of inertia was unsuitable for analysis. There is an offset in this series of tests which makes an analysis of these records break down. It is unclear whether this is due to an equipment malfunction or experimental technique, but, as other tests appear to be suitable, an equipment malfunction is suspected.

The effect of adding bilge keels to the model hull was to produce a sharp increase in the damping moment. This was to be expected from previous literature, Bolton [21]. It is unclear whether the addition of bilge keels changes the form of the damping, or, if so, to which form of damping it is changed. However, as indicated by Table 4.2.2, the roll decay tests of the R-Class icebreaker with bilge keels and the first moment of inertia show the velocity dependent damping forms as more viable than the angle dependent damping forms. This is slightly deceiving as, as mentioned previously, the velocity dependent damping forms can be considered as linear velocity damping with a coefficient that is a nonlinear function of the angle. This may suggest that the addition of the bilge keels produces a stronger nonlinear angle dependence of the damping moment. Figures 3.3.1-3, showing the change in energy per cycle for the R-Class icebreaker roll decay

tests, also suggest this stronger nonlinear angle dependence. In Figure 3.3.2 and Figure 3.3.3, for the tests with bilge keels, in the early cycles with the larger angles, the change in energy, and therefore the damping, is relatively large while the change in energy decreases nonlinearly through successive cycles. Figure 3.3.1, for the tests without bilge keels, this nonlinear decrease in the change in energy is not nearly as evident. Unfortunately, the limited number of cycles in the bilge keel roll decay records as well as the problems with the offsets in the records did not allow a clearer picture to be formed.

4.3 Analysis of Stillwater Roll Decay With Forward Speed

Stillwater roll decay tests with forward speed were performed on the R-Class icebreaker model in the second set of tests only. A speed range equivalent to a full scale speed range of from 2 to 16 knots was used with 2 knot increments. Fig. 4.3.1 shows the variation in the equivalent linear damping coefficient with speed.

As with the stillwater roll decay without forward speed, the equivalent linear damping coefficient increased with the addition of bilge keels and an increase in the natural frequency. As well, the equivalent linear damping coefficient increased with an increase in speed. This is to be expected from the literature, Schmitke [14]. The exact nature of the relationship between

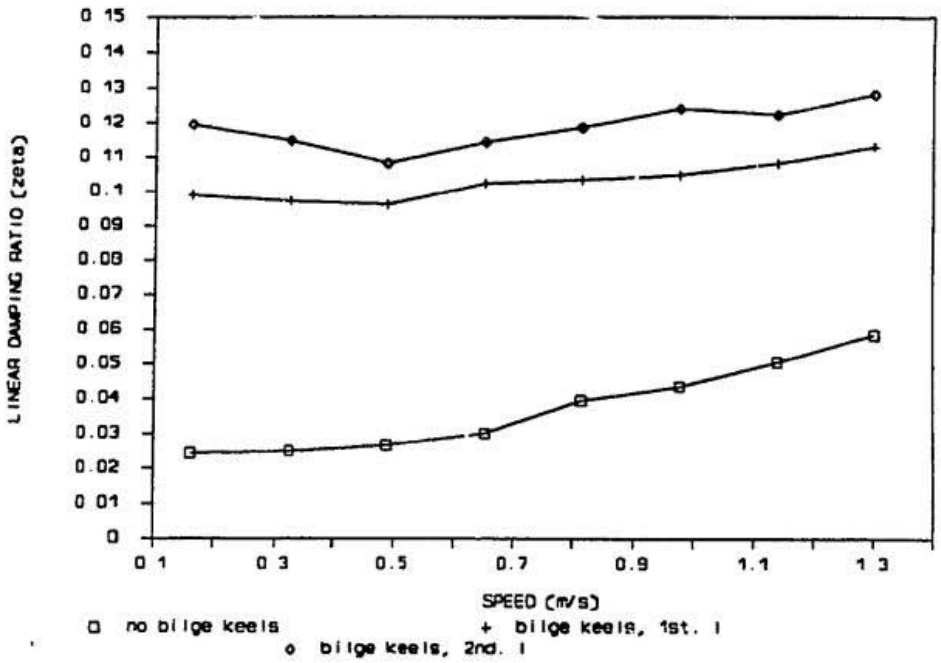

Figure 4.3.1
Damping coefficient vs speed for bilge keels (1st moment of inertia), bilge keels (2nd moment of inertia) and no bilge keels

the equivalent linear damping coefficient and the speed was not determined. However, a nonlinear form is suggested by Fig. 4.3.1.

A qualitative presentation of the damping coefficients used in the analyses is presented in Table 4.3.1-3. The tests without bilge keels show little or no angle dependence of the damping moment at slower speeds, from 2-12 knots, with perhaps a stronger angle dependence after 12 knots. The tests with bilge keels show almost the opposite trend. A stronger angle dependence is evidenced at the lower speeds from 2-8 knots, than at the higher speeds. The tests with bilge keels and the 2nd (smaller) moment of inertia show a stronger angle dependence than the tests with bilge keels and the 1st (larger) moment of inertia.

TABLE 4.3.1

Qualitative presentation of damping coefficients for whole roll decay with forward speed test
R-Class icebreaker tests without bilge keels

Knots	Damping coefficients: linear	velocity dependent: quadratic	velocity dependent: cubic	angle dependent: linear	angle dependent: quadratic
2	Y	Y	Y	-	-
4	Y	Y	Y	-	-
6	Y	Y	Y	Y	-
8	Y	Y	Y	-	-
10	Y	Y	Y	-	-
12	Y	Y	Y	-	-
14	Y	Y	Y	Y	-
16	Y	Y	Y	Y	Y

TABLE 4.3.2

Qualitative presentation of damping coefficients for whole roll decay with forward speed test
R-class icebreaker with bilge keels
1st moment of inertia

Knots	Damping coefficients: linear	velocity dependent: quadratic	velocity dependent: cubic	angle dependent: linear	angle dependent: quadratic
2	Y	Y	Y	Y	Y
4	Y	Y	Y	-	Y
6	Y	Y	Y	Y	Y
8	Y	Y	Y	Y	Y
10	Y	Y	Y	-	-
12	Y	Y	Y	-	-
14	Y	Y	Y	-	-
16	Y	Y	Y	Y	-

TABLE 4.3.3

Qualitative presentation of damping coefficients for whole roll decay with forward speed test
R-class icebreaker with bilge keels
2nd moment of inertia

Knots	Damping coefficients				
	linear	velocity dependent		angle dependent	
		quadratic	cubic	linear	quadratic
2	Y	Y	Y	Y	Y
4	Y	Y	Y	Y	Y
6	Y	Y	Y	Y	Y
8	Y	Y	Y	Y	Y
10	Y	Y	Y	-	-
12	Y	Y	Y	Y	-
14	Y	Y	Y	Y	Y
16	Y	Y	Y	Y	-

5.0 FORCED MOTION COMPARISON

In order to further validate the analyses, the damping coefficients were used to predict the forced motion response. For this validation, the damping coefficients derived from the tests without bilge keels of the R-Class icebreaker model in the second set of tests were used.

Forced roll tests in beam seas were performed for the following range of frequencies: 0.480 Hz, 0.500 Hz, 0.556 Hz, 0.600 Hz, 0.620 Hz. The average natural frequency of the model was 3.54 rad/sec or 0.563 Hz. A Runge-Kutta routine was used to predict the forced roll response using the following equation

$$\ddot{\phi} + 2\zeta\omega_n(\dot{\phi} + \epsilon|\dot{\phi}|\dot{\phi}) + \omega_n^2(\phi + a\phi^3 + b\phi^5) = F_o\cos(\omega_e t + \theta) \qquad 5.0.1$$

where ω_n = natural frequency of roll (rad/sec)
ζ = linear damping ratio
F_o = exciting moment due to waves
θ = phase angle of exciting moment
ω_e = wave forcing frequency

In order to obtain the exciting moment F_o and its phase angle θ , a strip theory programme was run using the offsets of the R-Class icebreaker. From the strip theory programme, non dimensional exciting moments for the

range of frequencies aforementioned were obtained as functions of the wave height, gravitational acceleration and the mass of the model. The wave heights were obtained from the wave probe data collected during the test. The phase angle of the exciting moment was also given by the strip theory programme and turned out to be either one tenth of a degree or zero and was therefore neglected.

The results of the forced response prediction and the comparison to the experimental forced response were not very good. There appears to be a shift to the right of the predicted response. This could be due to an error in the assumed values of the wave frequencies. If this shift is taken into account in the comparison, the predicted response is out by 24-35%. If the shift is not accounted for, the predicted response is out by up to 150%.

As a check, a simulated forced roll record was generated using the Runge-Kutta integration routine and the same damping coefficients as in the previously mentioned simulated roll decay curve, (See Sect. 3.4) with the following equation.

$$\ddot{\phi} + A\dot{\phi} + B|\dot{\phi}|\dot{\phi} + \omega_n^2\phi = 0.5\cos(\omega_e t) \qquad 5.0.2$$

where $A = 0.07$
$B = 0.50$
ω_n = natural frequency
ω_e = forcing frequency

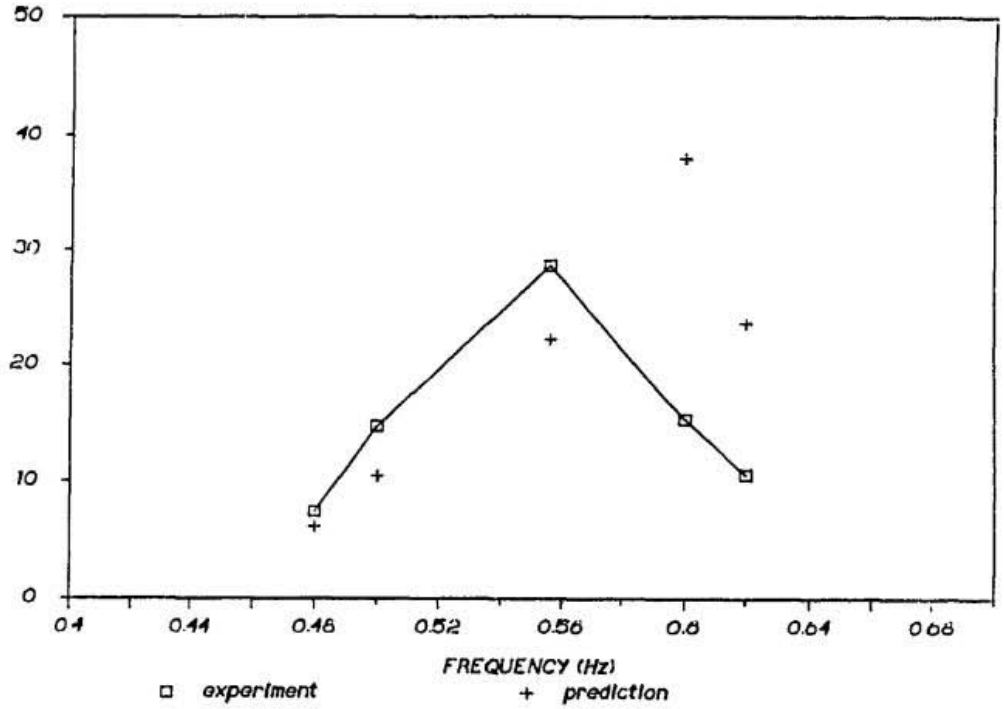

Figure 5.1
Predicted and experimental forced roll response in regular seas

Using the damping coefficients derived from the Energy method analysis, ie. A = 0.0685, B = 0.5009, the Runge-Kutta integration routine was again run and the results compared. The simulated forced motion record had an average response of 18.07 degrees. The Energy method forced motion record had an average response of 18.39 degrees. This was an error of 1.8% which was much closer than the error between prediction and experiment. This, however, was an ideal situation where the forcing moment was known exactly, the restoring moment was linear, the forcing and natural frequencies were known exactly and the form of the damping moment was known exactly.

For the comparison of prediction with experiment, errors are inherent in every step of the calculation. To begin with, for these tests, there was a discrepancy between the wave records as recorded by the two wave probes. One of the records was closer to the approximate wave heights as noted during the experiments and the amplitude of this record was used in the prediction. The wave amplitude has a major influence on the prediction as the exciting moment derived from the strip theory programme is directly dependent upon it. The wave probe data used are called into question simply because there is poor correspondence between the two wave probes. The damping moment form, although it gave the best prediction of the roll decay curve, is not necessarily the best form. Finally, due to the axis of

rotation being fixed, there is an extra exciting moment as the line of action of the sway force does not act through the axis of rotation. It is difficult to account for the variation of the line of action and magnitude of the sway force which introduces errors.

6.0 CONCLUSIONS

From the comparisons of the three methods considered, it was determined that the Perturbation method was the least favored of the three methods. This was due to the need to know initial estimates of the damping coefficients, the very narrow range within which the initial estimates had to lie, the inability to handle nonlinear restoring moments and its inapplicability for certain types of rolling motion, i.e. large nonlinearities and large amplitude motion. It also required the use of the roll decay peaks only, which necessitates the use relatively long roll decay records to obtain a reasonably accurate estimate.

Although the K.B. method uses roll peaks for its analysis also, unlike the Perturbation method it is easy to apply, requires no initial estimates and resulted in a more accurate prediction than the Perturbation method. However, it does not allow for the use of a nonlinear restoring moment which tends to reduce its accuracy for large amplitude motion. It also cannot separate the influence of angle dependent and velocity dependent components of the same order of magnitude. Based on the comparison of the predictions and the versatility of the methods, this method was considered better than the Perturbation method but not as good as the Energy method.

The Energy method was considered the best of the three methods for three main reasons. Firstly, the method uses the whole roll decay record, not just the peak values. Thus, shorter roll decay records can be used in the analysis. As well, the latter part of the roll decay records, with its attendant lower reliability, need not be used in the analysis. Secondly, the Energy method allows the use of a nonlinear restoring moment in the analysis. This provides a more accurate analysis of large amplitude motion. Thirdly, the influence of each component of the roll damping moment can be evaluated separately from the other components.

For these reasons, and the fact that the Energy method coefficients resulted in predictions of the simulated roll decay as good as, or better than either of the other two methods, the Energy method was considered the best of the three methods.

The Energy method tended to give more accurate results than the K.B. method for the tests without bilge keels, which had relatively large numbers of peak values, while the K.B. method gave equivalent results for the tests with bilge keels, which had relatively few peak values. As the K.B. method uses a least squares fit to the peak values, a good prediction by the K.B. method may be expected within the data range from the small number of peak values available for the tests with bilge keels.

The single cycle analysis of the roll decay record provided insights into the angle dependence of the roll damping moment. There is a definite relationship between the angle of roll and the equivalent linear damping coefficient as is seen in Figs. 4.1-8. There is an indication from the analysis of the tests with bilge keels that the angle dependence is nonlinear, but further investigation would be required to establish the form for these particular hulls. This angle dependence is supported by the viability of the angle dependent forms used in the analyses (See Table 4.1.2-7).

In the whole cycle analysis, the viability of the angle dependent forms is seen again, although now the predominant viable damping forms are the quadratic and cubic velocity dependent components. However, as is seen from equation (4.1.1), the velocity dependent components are actually nonlinear angle dependent models. The equivalent linear damping coefficient were viable for all the tests. The prediction outside the range of data was better using the velocity dependent coefficients, within 5-6% or less as the angle dependent components tended to overdamp outside the range of data. Within the data range, the predictions using the angle dependent terms were reasonable, being less than 10%. These results indicate that angle dependent terms should be included in an analysis of a roll decay record.

The analysis of the roll decay with forward speed records showed a strong dependence of the equivalent linear damping moment on the magnitude of the s$_t$ ed (See Fig. 4.3.1). This corresponds well with the literature, eg. Schmitke [14]. The roll damping moment with forward speed does not appear as strongly linearly angle dependent as the roll damping moment in stillwater when bilge keels are not present. With the addition of bilge keels, there appears to be a stronger angle dependence. As well, an increase in the natural frequency of roll seems to increase the angle dependence of the roll damping moment, although the specific form of the damping moment could not be determined.

7.0 REFERENCES and BIBLIOGRAPHY

1. The Papers of William Froude, The Institution of Naval Architects, London, 1955.

2. Haddara, M.R., "On The Stability of Ship Motion in Regular Oblique Waves", International Shipbuilding Progress, Vol. 18, No. 207, 1971.

3. Haddara, M.R., "A Note of the Effect of Damping Moment Form on Rolling", International Shipbuilding Progress, Vol. 31, No. 363, 1984.

4. Dalzell, J.F., "A Note on the Form of Ship Roll Damping", Journal of Ship Research, Vol. 22, No.3, 1978.

5. Spouge, J.R., Ireland, N. and Collins, J.P., "Large Amplitude Rolling Experiment Techniques", International Conference on the Stability of Ships and Ocean Vehicles, Gdansk, 1986.

6. Gawn, R.W.L., "Rolling Experiments with Ships and Models in Stillwater", The Institution of Naval Architects, Vol. 82, 1940.

7. Bass, D. and Haddara, M.R., "Nonlinear Models of Ship Roll Damping", International Shipbuilding Progress, Vol. 35, No. 401, 1988.

8. Roberts, J.B., "Estimation of Nonlinear Ship Roll Damping from Free Decay Data", Journal of Ship Research, Vol. 29, No. 2, 1985.

9. Mathisen, J.B., and Price, W.G., "Estimation of Ship Roll Damping Coefficients", Transactions of The Royal Institution of Naval Architects, 1984.

10. Marshfield, W.B., "Irregular Wave Experiments and Further Effects of Roll Damping and Bias", AMTE, Report R84219, June 1984.

11. Himeno, Y., "Prediction of Ship Roll Damping - State of the Art", University of Michigan, Dept. of Naval Architecture and Marine Engineering, Sept. 1981.

12. Haddara, M.R., "On Non Linear Rolling of Ships in Random Seas", International Shipbuilding Progress, Vol. 20, 1973.

13. Cardo, A., Ceschia, M., Francescutto, A. and Maergaj, R., "Effects of the Angle Dependent Damping on the Rolling Motion of Ships in Regular Beam Seas", International Shipbuilding Progress, Vol. 27, 1980.

7.0 REFERENCES and BIBLIOGRAPHY

1. The Papers of William Froude, The Institution of Naval Architects, London, 1955.

2. Haddara, M.R., "On The Stability of Ship Motion in Regular Oblique Waves", International Shipbuilding Progress, Vol. 18, No. 207, 1971.

3. Haddara, M.R., "A Note of the Effect of Damping Moment Form on Rolling", International Shipbuilding Progress, Vol. 31, No. 363, 1984.

4. Dalzell, J.F., "A Note on the Form of Ship Roll Damping", Journal of Ship Research, Vol. 22, No.3, 1978.

5. Spouge, J.R., Ireland, N. and Collins, J.P., "Large Amplitude Rolling Experiment Techniques", International Conference on the Stability of Ships and Ocean Vehicles, Gdansk, 1986.

6. Gawn, R.W.L., "Rolling Experiments with Ships and Models in Stillwater", The Institution of Naval Architects, Vol. 82, 1940.

7. Bass, D. and Haddara, M.R., "Nonlinear Models of Ship Roll Damping", International Shipbuilding Progress, Vol. 35, No. 401, 1988.

8. Roberts, J.B., "Estimation of Nonlinear Ship Roll Damping from Free Decay Data", Journal of Ship Research, Vol. 29, No. 2, 1985.

9. Mathisen, J.B., and Price, W.G., "Estimation of Ship Roll Damping Coefficients", Transactions of The Royal Institution of Naval Architects, 1984.

10. Marshfield, W.B., "Irregular Wave Experiments and Further Effects of Roll Damping and Bias", AMTE, Report R84219, June 1984.

11. Himeno, Y., "Prediction of Ship Roll Damping - State of the Art", University of Michigan, Dept. of Naval Architecture and Marine Engineering, Sept. 1981.

12. Haddara, M.R., "On Non Linear Rolling of Ships in Random Seas", International Shipbuilding Progress, Vol. 20, 1973.

13. Cardo, A., Ceschia, M., Francescutto, A. and Maergaj, R., "Effects of the Angle Dependent Damping on the Rolling Motion of Ships in Regular Beam Seas", International Shipbuilding Progress, Vol. 27, 1980.

14. Schmitke, R.T., "Ship Sway, Roll and Yaw Motions in Oblique Seas", Trans. SNAME, Vol. 86, 1978.

15. Salvisen, N. Tuck, E.O. and Faltinsen, O., "Ship Motions and Sea Loads", Trans. SNAME, Vol. 78, 1970.

16. Obadasi, A.Y., "Hydrodynamic Reaction to Large Amplitude Rolling Motion", International Shipbuilding Progress, Vol. 28, No. 320, 1984.

17. Blagoveshchensky, S.N., "Theory of Ship Motions", (two volumes), Dover Publications, New York, 1962.

18. Obadasi, A.Y., "Ultimate Stability of Ships", Transactions of The Royal Institution of Naval Architects, 1977.

19. St.Denis, M., Pierson, W.J., "On The Motion of Ships in Confused Seas", Trans. SNAME, Vol. 61, 1953.

20. Tasai, F., "On the Swaying, Yawing and Rolling Motions of Ships in Oblique Waves", International Shipbuilding Progress, Vol. 14, No. 153, 1967.

21. Bolton, W.E., "The Effects of Bilge Keel Size on Roll Reduction", Admiralty Experiment Works, Report 19/72, 1972.

22. Lugovski, V.V., Kholodilin, A.M., Shipukov, O.G., "Experimental Study of Scale Effect on Evaluation of Roll Damping Action of Bilge Keels", Contributed paper to 14th ITTC Seakeeping Committee, 1975.

23. Ueno, K., "Influence of the Surface Tension of the Surrounding Water Upon the Free Rolling of Model Ships", Report, Research Institute for Applied Mechanics, Kyushu University, 1949.

24. Vassilopoulos, L., "Ship Rolling at Zero Speed in Random Beam Seas With Non Linear Damping and Restoration", Journal of Ship Research, Vol. 15, No. 4, Dec. 1971.

25. Mandel, P., "Some Hydrodynamic Aspects of Appendage Design", Trans. SNAME, Vol. 61, 1953.

26. Gersten, A., "Effect of Forward Speed on Roll Damping Due to Viscosity and Eddy Generation", NSRDC Report 2725, July 1968.

27. Laurich, P.H., "The Selspot System", National Research Council of Canada, Ottawa, Technical Report No. 23187, 1987.

28. Ikeda, Y., Tanaka, N., Himeno, Y., "Effect of Hull Form and Appendage on Roll Motion of Small Fishing Vessel", Second International Conference on Stability of Ships and Ocean Vehicles, Tokyo, Oct. 1982.

29. Bass, D., Haddara, M.R., "On the Modelling of the Nonlinear Damping Moment for the Rolling Motion of a Ship", IASTED, Identification, Modelling and Simulation, Paris, France, June 22-24, 1987.

30. Bryan, G. H., "The Action of Bilge Keels", Transactions of the Royal Institution of Naval Architects, Vol. 42, 1900

31. Haddara, M. R., "Study of the Stability of the Mean and Variance of Rolling Motion in Random Waves", Proceedings of the International Conference on Stability of Ships and Ocean Vehicles, University of Strathclyde, Glasgow, March 1975

32. Graham, R., "The Effects of Hull Form Variations on the Roll Damping of Warships", Naval Engineers Journal, Sept. 1987

33. Kerwin, J. E., "Notes on Rolling in Longitudinal Wave", International Shipbuilding Progress, Vol. 2, 1955